

Power-type derivatives for rough volatility with jumps

Weixuan Xia*

2020

Abstract

In this paper we propose an efficient pricing-hedging framework for volatility derivatives which simultaneously takes into account path roughness and jumps. Instead of dealing with log-volatility, we directly model the instantaneous variance of a risky asset in terms of a fractional Ornstein-Uhlenbeck process driven by an infinite-activity Lévy subordinator, which is shown to exhibit roughness under suitable conditions and also eludes the need for an independent Brownian component. This structure renders the characteristic function of forward variance obtainable at least in semi-closed form, subject to a generic integrable kernel. To analyze financial derivatives, primarily swaps and European-style options, on average forward volatility, we introduce a general class of power-type derivatives on the average forward variance, which also provide a way of adjusting the option investor's risk exposure. Pricing formulae are based on numerical inverse Fourier transform and, as illustrated by an empirical study on VIX options, permit stable and efficient model calibration once specified.

MSC2020 Classifications: 60E10; 60G22; 60J76

JEL Classifications: C65; G13

KEY WORDS: Rough volatility; volatility jumps; forward variance; power-type derivatives

1 Introduction

“Rough volatility” is a relatively new and yet already familiar jargon that has come into being in the financial world since the pioneering research work of [Gatheral et al, 2018] [11], which provided important empirical evidence suggesting rough sample paths of volatility observed in high-frequency financial time series and thus the presence of short-term dependence. Over the past three years, a good number of works have also been devoted into empirical justifications of the presence of rough volatility in various asset types. To name a few, [Livieri et al, 2018] [21] confirmed the existence of rough volatility by studying implied volatility-based approximations of spot volatility of the S&P500 index, [Takaishi, 2020] [32] collected further evidence supporting volatility roughness in the cryptocurrency (in particular Bitcoin) market, and [Da Franseca and Zhang, 2019] [7] even demonstrated that roughness is also present in the VIX index.

Although the introduction of rough volatility has been a successful reproducer of stylized features of historical volatility of asset prices, a series of difficulties have arisen in the

*Correspondence address: Department of Finance, Boston University Questrom School of Business. Email: gabxia@bu.edu.

meantime because of the loss of Markov and semimartingale properties. As a result, when developing pricing-hedging techniques accounting for rough volatility one will probably sojourn at Monte-Carlo simulation methods, whereas the inaccessibility of infinitesimal generators has disabled methods associated with the Feynman-Kac formula. So far, simulation-based pricing-hedging methods have already been studied in depth; for example, [Jacquier et al, 2018] [16] adopted a hybrid simulation scheme for the calibration of the rough Bergomi model initially proposed in [Bayer et al, 2016] [3] on VIX futures and options. On the other hand, under the so-called “rough Heston model” which is constructed from a stationary power-type kernel and belongs to the family of affine Volterra processes discussed in [Jaber et al, 2019] [15] (see also [Gatheral and Keller-Ressel, 2019] [12]), characteristic function-based pricing methods were derived in [El Euch and Rosenbaum, 2019] [9] which depend, partially, on solving a fractional Riccati equation, where their applicability was also demonstrated by a simple calibration exercise on S&P500 implied volatility surfaces; the paper [El Euch and Rosenbaum, 2018] [8] by the same authors considered from a theoretical standpoint similar hedging problems, after being able to write the characteristic function of the log asset price in terms of a functional of its corresponding forward variance curve. We also notice the up-to-date work of [Horvath et al, 2020] [14], which highlighted a martingale framework using forward variance curves in the goal of studying volatility options. It is worth mentioning that all these recent works have universally emphasized the role of a Brownian motion while paying little attention to jumps in the asset prices and their volatility, which are, of course, thought to complicate the pricing problems to great extent. For instance, the aforementioned Riccati equation will turn into an integro-differential equation entailing more computationally expensive numerical schemes and the resulting model distributions will no longer be stable but subject to substantial changes under integral operations.

All relevant models aside, one should however bear in mind that the main idea behind rough volatility is the exhibition of short-term dependence, or more precisely, rapidly decaying autocorrelation near the origin, rather than an inherent reliance on Brownian sample paths, or path continuity, which characteristic is at bottom an estimation assumption imposed in [Gatheral et al, 2018] [11] and deemed nonessential. In fact, extensive use of the Brownian motion in the cited literature is understandably an act of simplicity, mainly due to log-instantaneous volatility shown to be empirically close to normally distributed. On the other hand, disregarding the exclusive use of the Brownian motion sheds light upon another important aspect - the presence of volatility jumps. In a semimartingale setting, this would send us back to the work of [Todorov and Tauchen, 2011] [34], which, by inferring from high-frequency VIX index data the activity level of some presumed mean-reverting instantaneous variance model, showed that stock market volatility should be most suitably depicted as a purely discontinuous process without a Brownian component. Notably, this concern may not exist anymore in a non-semimartingale model with frictions, as pointed out in the same paper; in short, the activity level of the process can be flexibly adjusted according to the controlling fraction parameter. For this reason, inclusion of volatility jumps in a model that is already fractional has seemingly been considered insignificant and neglected for investigation. Nevertheless, since increased activ-

ity levels are an inevitable consequence of rough sample paths, using a fractional Brownian motion with a fraction parameter less than 1 only increases the vibrancy of the resulting variance process, which somewhat turns aside the empirical findings of [Todorov and Tauchen, 2011] [34]. In connection with this, we expect that replacing the Brownian motion with a purely discontinuous component, which is less vibrant, is able to strike a balance between these two important aspects (short-term dependence and volatility jumps) and eventually yield desirable modeling outcomes.

These inspire us to take on a new path deviating from the use of a fractional Brownian motion in the establishment of rough volatility and switch to purely discontinuous square-integrable Lévy processes of infinite activity. In more detail, we want to propose a general framework for the instantaneous variance based on a generalized fractional Ornstein-Uhlenbeck process subject to an integrable and possibly non-stationary kernel; a key feature of this formulation is that it is not derived from taking natural logarithm but yet is capable of simultaneously capturing path roughness and possible jumps in the instantaneous variance. Needless to say, despite that inclusion of jumps may not result in significant improvement of the model fit of volatility distributions observed at high frequencies, as noted in [Gatheral et al, 2018, Sect. 6] [11], it is undoubtedly innocuous and the model distribution in logarithm can also become arbitrarily close to normality by properly adjusting its scale parameter, thanks to the central limit theorem. On the contrary, introducing jumps into the instantaneous variance gives rise to an analytically tractable structure for the characteristic function of the average forward volatility, thus facilitating the pricing and hedging of corresponding financial derivatives. The only inexact measure to be taken, however, is a parametric kernel approximation, and can be looked upon as a replacement of the geometric-averaging approximation adopted in [Horvath et al, 2020, Eq. (16)] [14]. To be more specific, for a certain investment horizon the average forward volatility can be decently approximated by a forward volatility with an unknown window to be treated as a constrained parameter, and this does not pose any problems as long as the kernel satisfies a certain differentiability condition.

Besides, although our main results are given under a general setting, attention will be drawn to three particular types of stationary kernels, all of which are comfortable to work with and have their own advantages. While the first type is recognized for its incommensurable simplicity, the second is compatible with the transformation of the instantaneous variance dynamics into a usual Ornstein-Uhlenbeck process driven by a fractional Lévy process. The third type, being part of our innovation, is arguably a result of reverse engineering and designed specifically to ensure a closed-form characteristic function - a truly desirable tool that underlies efficient calibration. Remarkably, our objective is not to compare the overall suitability of different types of kernels, but rather, to seek one that facilitates numerical implementation to the greatest degree; in fact, all these three types are very similar in shape.

Our ultimate interest in the present paper lies in analyzing European-style financial derivatives written on the average forward volatility, such as the VIX index, including swaps and options. Under the proposed rough-volatility framework, we obtain pricing-hedging formulae for a more general class of power-type derivatives, which raise the un-

derlying volatility or the standard option payoff to a certain nonnegative power, and can thus be applied to conveniently adjust the derivative investor's risk exposure. While these derivatives are rather newfangled in the volatility market, their counterparts written on equity prices have been thoroughly studied already and one is referred to [Raible, 2000] [28] and [Xia, 2017] [38] on single-asset options and [Blenman and Clark, 2005] [4], [Wang, 2016] [35], and [Xia, 2019] [39] on exchange options. The proposed pricing-hedging formulae will make extensive use of the incomplete gamma function but only involve one numerical Fourier-type integral, and thus are very convenient to implement in practice.

The remainder of this paper is organized as follows. In Section 2 we establish our model framework starting from a fractional instantaneous variance dynamics and provide a comprehensive analysis of its properties, including covariance function and path regularity, and then give an integral representation for the characteristic function of the average forward variance. Some simulation techniques are discussed in Section 3, with some pertinent convergence results. Section 4 contains our new pricing-hedging formulae for power-type derivatives which naturally generalize standard volatility derivatives, initiating our empirical study based on the VIX index in Section 5. Moreover, we also provide some insight into how the model framework may be further extended to accommodate the presence of rough volatility of volatility in Section 6 by means of a stochastic time change argument, in catering for the noted finding of [Da Franseca and Zhang, 2019] [7]. Conclusions are drawn in Section 7 and all mathematical proofs presented in the end.

2 Construction of rough volatility with jumps

2.1 Fractional Lévy processes

We begin by synthesizing some crucial ingredients of a non-Gaussian fractional Lévy process, which are necessary for establishing a model for the instantaneous variance of a risky asset whose sample paths have roughness and jump features. Of course, allowing for positivity of the instantaneous variance the background-driving Lévy process must be nonnegative, i.e., a subordinator.

To this end, consider a continuous-time stochastic basis $\mathfrak{S} := (\Omega, \mathcal{F}, \mathbb{P}; \mathbb{F} \equiv \{\mathcal{F}_t\}_{t \geq 0})$, where the filtration \mathbb{F} is assumed to satisfy the usual conditions. Let $X \equiv (X_t)$ be an adapted and square-integrable Lévy subordinator supported on \mathfrak{S} , which is exclusively characterized by a Poisson random measure N defined on $(\mathbb{R}_{++}, \mathbb{R}_+)$. According to the Lévy-Khintchine representation, X_1 has the characteristic exponent

$$\log \phi_{X_1}(l) := \log \mathbb{E}[e^{ilX_1}] = \int_{0+}^{\infty} (e^{ilz} - 1) \nu(dz), \quad l \in \mathbb{R},$$

where i denotes the imaginary unit and ν is the intensity measure associated with N . For practicality we impose the assumption that ν is non-atomic so that the law of X_1 is absolutely continuous with respect to Lebesgue measure and we denote by $\xi_1 := \mathbb{E}[X_1] > 0$ and $\xi_2 := \mathbb{E}[X_1^2] > 0$ its first two moments. Since X has independent and stationary incre-

ments, it has the familiar covariance function, for any $u > 0$,

$$\text{Cov}[X_t, X_{t+u}] = \xi_2 t - \xi_1^2 t(t+u).$$

For a continuously differentiable¹ kernel $g \in \mathcal{C}^{(1,1)}$ defined in the domain $\{(t, s) : t > 0, s \in [0, t]\}$ satisfying the integrability condition

$$\int_0^t g^2(t, s) ds < \infty, \quad \forall t > 0,$$

we then define the fractional Lévy process via the following Volterra-type stochastic integral,

$$X_t^{(g)} := \int_0^t g(t, s) dX_s = \int_0^t \int_{0+}^\infty g(t, s) z N(dz, ds), \quad t \geq 0. \quad (1)$$

With this representation, for any $t, u > 0$, it is easy to see that $\mathbb{E}[X_t^{(g)}] = \xi_1 \int_0^t g(t, s) ds$ and, by using the Lévy-Itô isometry (see, e.g., [Lyasoff, 2017, Sect. 16.32] [22]), the covariance function of the centered process $(X_t^{(g)} - \mathbb{E}[X_t^{(g)}])$ takes the following form,

$$\mathbb{E}[X_t^{(g)} X_{t+u}^{(g)}] = \xi_2 \int_0^t g(t, s) g(t+u, s) ds.$$

Notably, if $\lim_{s \nearrow t} g(t, s) = \infty$ for every $t > 0$, then the integral $\int_0^t g^{(0,1)}(t, s) ds$ is divergent for every $t > 0$. In this case, $X^{(g)}$ exhibits short-term dependence with rough sample paths in the sense that there exists $\varpi \in (0, 1)$ such that

$$\mathbb{E}[X_t^{(g)} X_{t+u}^{(g)}] = \mathbb{E}[X_t^{(g)^2}] + \xi_2 C(t) u^\varpi + O(u),$$

where $\mathbb{E}[X_t^{(g)^2}] = \xi_2 \int_0^t g^2(t, s) ds$ by the dominated convergence theorem and $C(t)$ is some constant depending only on $t > 0$.

To give a few examples, the Molchan-Golosov kernel ([Molchan and Golosov, 1969] [26]) reads

$$g(t, s) = (t-s)^{d-1} {}_2F_1\left(-d, d-1; d; -\frac{t-s}{s}\right), \quad (2)$$

for some fraction parameter $d \in (1/2, 3/2)$, where ${}_2F_1(\cdot, \cdot; \cdot; \cdot)$ is the Gauss hypergeometric (2, 1) function ([Abramowitz and Stegun, 1972, Sect. 15] [1]) and which is non-stationary. We note that the specific form (2) was initially chosen in [Jost, 2006] [17] in an attempt to match the Weyl integral representation of a fractional Brownian motion living in real-valued time used in [Mandelbrot and van Ness, 1968] [23]. It was shown in [Tikanmäki and Mishura, 2011] [33], however, that such transformation does not necessarily lead to the same finite-dimensional distribution in the more general case of fractional Lévy processes. Another popular choice of g is the following obviously stationary and yet structurally much simpler Riemann-Liouville kernel²,

$$g(t, s) \equiv g(t-s) = \frac{(t-s)^{d-1}}{\Gamma(d)}, \quad (3)$$

¹Continuous differentiability is a highly desirable property of the kernel for modeling purposes, hence assumed throughout this paper. Intuitively, by ruling out kinks and discontinuities it ensures that the frictions brought by g do not have sudden changes. However, it is not required for defining fractional Lévy subordinators and thus not to be comprehended as any implicit assumption for the ongoing analysis.

²The same kernel was used in [El Euch, 2018] [8] and [El Euch, 2019] [9] in constructing the (generalized) rough Heston model.

for $d > 1/2$, where $\Gamma(\cdot)$ denotes the usual gamma function. In particular, with (3) the fractional process $X^{(g)}$ can also be understood as a consequence of repeated path integration of the subordinator X , i.e., for $d \in \mathbb{N}_{++} \equiv \mathbb{N} \setminus \{0\}$,

$$X_t^{(g)} = \underbrace{\int \cdots \int_0^t}_{d} X_s \underbrace{ds \cdots ds}_d, \quad (4)$$

which can be extended through Cauchy's repeated integration formula. Of course, for this special choice roughness is only present if $d \in (1/2, 1)$, while it also has the obvious drawback, compared to the Molchan-Golosov kernel, that the resulting fractional process fails to have stationary increments.

In any case, a well-suited candidate for X , having infinitely many jumps on compact time intervals, can simply be a one-sided tempered stable process, i.e., a tempered stable subordinator, which has three parameters - $a > 0$, $b > 0$ and $c \in (0, 1)$, leading to the following characteristic exponent,

$$\log \phi_{X_1}(l) = a\Gamma(-c)((b - il)^c - b^c), \quad l \in \mathbb{R}, \quad (5)$$

so that $\nu(dz) = ae^{-bz}/z^{c+1} \mathbb{1}_{(0, \infty)}(z)dz$, for $z > 0$, which is clearly an infinite measure. By taking $c \searrow 0$ and $c = 1/2$, one recovers the well-known gamma process and inverse Gaussian process, respectively. In particular, in the former case we have $\log \phi_{X_1}(l) = -a \log(1 - il/b)$. With (5) it is also straightforward to verify that $\xi_1 = a\Gamma(1 - c)/b^{1-c}$ and $\xi_2 - \xi_1^2 = a\Gamma(2 - c)/b^{2-c}$. For more concrete properties of the tempered stable process one may refer to [Rosiński, 2007] [29] and [Küchler and Tappe, 2013] [19]; see also [Schoutens, 2003, Sect. 5.3] [30] for an overview.

2.2 Instantaneous variance

Let us consider, instead of the natural logarithm of the instantaneous volatility of a risky asset, the instantaneous variance process, denoted $V \equiv (V_t)$. Intuitively speaking, our idea is to express V as a Volterra-type stochastic integral, up to shifting and positive scaling, analogous to the fractional Lévy process $X^{(g)}$ in (1) with a suitable kernel chosen to allow for short- or long-term dependence as well as long-term mean reversion. This is done by assuming the following fractional Ornstein-Uhlenbeck structure,

$$V_t = V_0 e^{-\kappa t} + \bar{V}(1 - e^{-\kappa t}) + X_t^{(h)}, \quad t \geq 0, \quad (6)$$

where $\kappa > 0$ specifies the reversion speed and $\bar{V} \geq 0$ a universal reversion level, and h is a continuously differentiable kernel having a power-law left tail and a quasi-exponential right tail,

$$h(t + u, t) = \begin{cases} O(u^{d-1}), & \text{as } u \searrow 0, \\ O(e^{-\kappa u} u^{(d-1)^+}), & \text{as } u \rightarrow \infty, \end{cases} \quad \forall t > 0, \quad (7)$$

for a fraction parameter $d > 1/2$, where $(\cdot)^+$ denotes the positive part. This condition subtly embodies the intuition of introducing frictions into V without jeopardizing its mean-

reverting property, and it automatically ensures that (6) is well defined because

$$\sup_{t>0} \int_0^t h^2(t, s) ds < \infty.$$

Besides, we assume that $V_0 > 0$ has a known value. In fact, if (7) holds with $d \in (1/2, 1)$, then V exhibits mean reversion in the long term but is simultaneously allowed to have short-term dependence. As before, with the Lévy-Itô isometry the centered process $(V_t - \mathbb{E}[V_t])$ is seen to have the covariance function equal to

$$\mathbb{E}[X_t^{(h)} X_{t+u}^{(h)}] = \xi_2 \int_0^t h(t, s) h(t+u, s) ds,$$

for any $u > 0$, which generally depends on $t > 0$. Under (7), if $d < 1$ then $\lim_{s \nearrow t} h(t, s) = \infty$ for any $t > 0$ and there exists $C(t) \in \mathbb{R}$ depending only on t such that

$$\mathbb{E}[X_t^{(h)} X_{t+u}^{(h)}] = \mathbb{E}[X_t^{(h)^2}] + \xi_2 C(t) u^{2d-1} + O(u), \quad \text{as } u \searrow 0, \quad (8)$$

with $\mathbb{E}[X_t^{(h)^2}] = \xi_2 \int_0^t h^2(t, s) ds$. In this case, the covariance function is rough at the origin and V does exhibit short-term dependence. On the other hand, with the right-tail behavior in (7) V always reverts to a positive mean in the long term, in that

$$\lim_{t \rightarrow \infty} \mathbb{E}[V_t] = \bar{V} + \xi_1 \lim_{t \rightarrow \infty} \int_0^t h(t, s) ds > 0.$$

The general construction of the fractional Ornstein-Uhlenbeck process in (6) is actually motivated by the recipe used in [Wolpert and Taqqu, 2004, Sect. 3] [37] based on repeated integration, where h is specialized as the product of a usual exponential kernel and the Riemann-Liouville kernel,

$$h(t, s) \equiv h(t-s) = \frac{e^{-\kappa(t-s)}(t-s)^{d-1}}{\Gamma(d)}, \quad (9)$$

which is clearly strictly positive and will be referred to as the type-I kernel. A remarkable difference is, however, that we have abandoned negative time by assuming that the instantaneous variance process is only observed starting from time 0.

Indeed, the structure (6) represents a wide range of approaches towards achieving path roughness and mean reversion at the same time, while it gives rise to an Ornstein-Uhlenbeck process driven by a fractional Lévy process, i.e., the structure used in [Garnier and Sølna, 2018] [10], by choosing

$$h(t, s) = g(t, s) - \kappa \int_s^t e^{-\kappa(t-v)} g(v, s) dv, \quad (10)$$

where g is the kernel mentioned in the previous section, esp. (1). Note that with an application of Itô's formula and the Fubini-Tonelli theorem (6) is reformatted into

$$V_t = V_0 e^{-\kappa t} + \bar{V}(1 - e^{-\kappa t}) + \int_0^t e^{-\kappa(t-s)} dX_s^{(g)}, \quad (11)$$

which is the solution of the fractional stochastic integral equation

$$V_t = \kappa \int_0^t (\bar{V} - V_s) ds + X_t^{(g)}.$$

Also, we remark that, due to the condition (7), the second term on the left-hand side of (11) is bounded for every fixed $t > 0$, so that $\lim_{s \nearrow t} h(t, s)/g(t, s) > 0$ exists, provided $\lim_{s \nearrow t} g(t, s) = \infty$ for any $t > 0$. This means that if g is chosen in such a way that the sample paths of $X^{(g)}$ exhibit short-term dependence, then those of V must also exhibit short-term dependence, and in fact, the path roughness of V and $X^{(g)}$ must be of the same degree. If g is further taken to be the stationary Riemann-Liouville kernel, then by straightforward calculations (10) yields the following type-II kernel which also happens to be stationary³,

$$h(t, s) \equiv h(t - s) = \frac{(t - s)^{d-1} + (-\kappa)^{1-d} e^{-\kappa(t-s)} (\Gamma(d) - \Gamma(d, -\kappa(t-s)))}{\Gamma(d)}, \quad (12)$$

where $\Gamma(\cdot, \cdot)$ denotes the upper incomplete gamma function, and the correlation structure (8) can be made more precise with $\mathbb{E}[X_t^{(h)2}] = \xi_2 \int_0^t h^2(s) ds$ and some

$$C(t) \in \frac{\Gamma(1-2d) \sin(\pi d)}{\pi \Gamma^2(d)} \times (e^{-2\kappa t}, 1), \quad (13)$$

which only depends on t . This shows that roughness is established if and only if $d \in (1/2, 1)$. Also, the long-term mean is given by $\lim_{t \rightarrow \infty} \mathbb{E}[V_t] = \bar{V} + \xi_1 \kappa^{-d}/2$.

Of course, with the type-I kernel (9), it is not possible to interpret V as an Ornstein-Uhlenbeck process driven by a fractional Lévy process. Nonetheless, V can still have short-term dependence, i.e., for $d \in (1/2, 1)$,

$$\frac{\mathbb{E}[X_t^{(h)} X_{t+u}^{(h)}]}{\xi_2} = \frac{t^{2d-1}}{(2d-1)\Gamma^2(d)} + C(t)u^{2d-1} + O(u), \quad \text{as } u \searrow 0,$$

which uses (13). The long-term mean is substantially no different: $\lim_{t \rightarrow \infty} \mathbb{E}[V_t] = \bar{V} + \xi_1 \kappa^{-d}$.

As an important aspect of our innovation, for $d \in (1/2, 1)$ generating short-term dependence we propose to construct h by combining the scaled exponential kernel and the Riemann-Liouville kernel in a piecewise fashion, i.e.,

$$h(t, s) \equiv h(t - s) = \begin{cases} \frac{(t - s)^{d-1} - \tau^{d-1}}{\Gamma(d)} + \theta e^{-\kappa \tau} & \text{if } t - s < \tau, \\ \theta e^{-\kappa(t-s)} & \text{if } t - s \geq \tau, \end{cases} \quad (14)$$

where $\tau > 0$ is some time threshold separating the power-law and exponential parts of the kernel and $\theta > 0$ is some scaling factor. In catering for continuous differentiability, τ solves the transcendental equation

$$e^{\kappa \tau} \tau^{d-2} = -\kappa \theta \Gamma(d-1). \quad (15)$$

³Unlike the type-I kernel, the type-II kernel is not necessarily strictly positive, though the resulting process V obviously is.

In order for (15) to be solvable on \mathbb{R}_{++} , θ has to satisfy the constraint

$$\theta \geq -\frac{1}{\kappa\Gamma(d-1)}\left(\frac{2-d}{e\kappa}\right)^{d-2}, \quad (16)$$

under which

$$\tau = \frac{d-2}{\kappa} W_i\left(\frac{\kappa}{d-2}(-\kappa\theta\Gamma(d-1))^{1/(d-2)}\right), \quad i \in \{-1, 0\}, \quad (17)$$

with $W(\cdot)$ being the Lambert W function, a.k.a. the product logarithm (see [Corless et al, 1996] [6]). Note that the two solutions in (17) coincide if and only if equality holds in (16). We will refer to (14) as the type-III kernel. Of course, a downside of such piecewise construction is its incompatibility with differentiability at τ if one requires long-term dependence ($d > 1$), in which case (15) has no positive solutions. In particular, if we take θ to be exactly the lower bound in (16) and specify (14) accordingly, then $\tau = (2-d)/\kappa$ and the type-III kernel is uniquely parameterized by κ and d and reads

$$h(t-s) = \begin{cases} \frac{(t-s)^{d-1} - ((2-d)/\kappa)^{d-1}}{\Gamma(d)} - \frac{e^{d-2}}{\kappa\Gamma(d-1)}\left(\frac{2-d}{e\kappa}\right)^{d-2} & \text{if } t-s < \frac{2-d}{\kappa}, \\ -\frac{e^{-\kappa(t-s)}}{\kappa\Gamma(d-1)}\left(\frac{2-d}{e\kappa}\right)^{d-2} & \text{if } t-s \geq \frac{2-d}{\kappa}, \end{cases} \quad (18)$$

which will play an important role during our implementation. With (18), we have in (8) that $C(t) \equiv C = \Gamma(1-2d)\sin(\pi d)/(\pi\Gamma^2(d))$ while the long-term mean becomes

$$\lim_{t \rightarrow \infty} \mathbb{E}[V_t] = \bar{V} + \frac{\xi_1(4-d)}{d(2-d)^3\Gamma(d-2)}\left(\frac{2-d}{\kappa}\right)^d > 0.$$

Using $\kappa = 5$ and $d = 0.6$, Figure 1 on the next page compares the three types of kernels (9), (12) and (18) over the unit time interval, from which it is clear that they share the same right-tail behavior and hence generate the same degree of roughness. In fact, with $d < 1$ the type-I and type-III kernels are both monotone whereas the type-II kernel need not be. Also, we note that in this illustration the two parts of the type-III kernel are separated at $1 - \tau = 0.72$. For $d = 1.1$, similar comparison is made between (9) and (12).

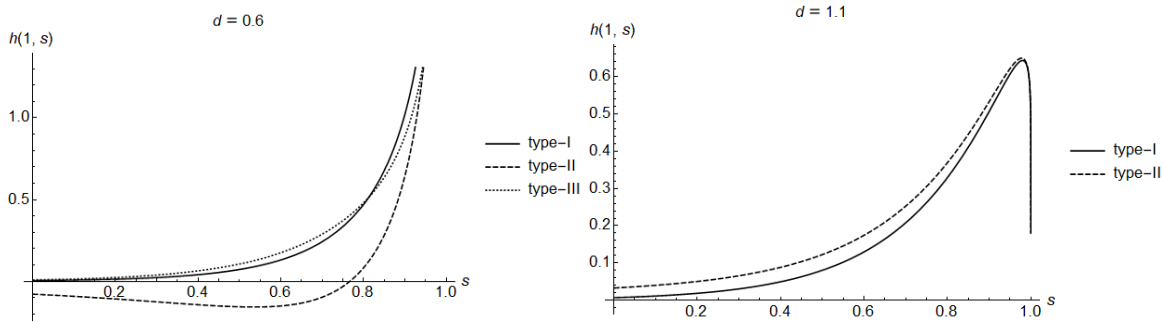


Figure 1: Comparison of kernels

On a different note, despite that by the formulation (6) V lacks increment stationarity, there is comprehensibly no negative impact placed on characteristic function-based model calibration.

In the next proposition we give some partial results on the regularity of the sample paths of V . Indeed, even from its appellation the interpretation of the so-called “path roughness” is not confined to the involvement of short-term dependence, but should be linked to how irregular the paths may become. Allowing for practicality, we focus on the case of an infinite Lévy measure ν .

Proposition 1. *Assume $\nu(\mathbb{R}_{++}) = \infty$ and (6). For any fixed $T > 0$ we have the following three assertions.*

(i) *If $d > 1$, then the sample paths of V are a.s. continuous with a.s. zero quadratic variation over $[0, T]$.*

(ii) *If $d = 1$, then the sample paths of V are a.s. discontinuous with a.s. finite quadratic variation over $[0, T]$.*

(iii) *If $1/2 < d < 1$, then the sample paths of V are a.s. discontinuous and unbounded with a.s. infinite quadratic variation over $[0, T]$.*

Notably, for $d > 1$, the sample paths of V are smoothed in a way that all the jumps generated by X are expunged and, as will be seen in the proof in Section 8.1, they are actually Hölder-continuous for certain exponents. On the other hand, in the situation of assertion (iii), V can have infinitely large jumps, so that its sample paths form maps from $[0, T]$ to $[0, \infty]$. We stress, however, that this will not be a problem for modeling in practice because V_t is a.s. finite for any fixed $t \geq 0$ and in fact, it has a finite variance. Of course, for the critical value $d = 1$, V only exhibits mean reversion. For the type-I and type-II kernels it can be easily verified that in the case $d = 1$ V is exactly the usual Lévy-driven Ornstein-Uhlenbeck process and for the type-III kernel this is also true in the limit as $d \nearrow 1$.

In any case, letting $t_0 \in [0, t]$ be a fixed time point, we can recast (6) conditional on \mathcal{F}_{t_0} as

$$V_t = V_0 e^{-\kappa t} + \bar{V}(1 - e^{-\kappa t}) + \int_0^{t_0} h(t, s) dX_s + \int_{t_0}^t h(t, s) dX_s \quad (19)$$

or equivalently,

$$V_t = V_{t_0} e^{-\kappa(t-t_0)} + \bar{V}(1 - e^{-\kappa(t-t_0)}) + \int_0^{t_0} (h(t, s) - e^{-\kappa(t-t_0)} h(t_0, s)) dX_s + \int_{t_0}^t h(t, s) dX_s. \quad (20)$$

Notably, the first integral on the right-hand side of (20) indicates that V cannot be a Markov process or a semimartingale in general. In fact, it is so if and only if h is chosen such that $h(t, s) - e^{-\kappa(t-t_0)} h(t_0, s) \equiv 0$, a clear contradiction with the inclusion of short-term dependence; for instance, with the aforementioned three types of kernels this integral does not vanish. With the loss of the Markov property, it is oftentimes more comfortable to work directly with (19). The conditional mean and covariance of the instantaneous variance can be directly written down. For any fixed $t > t_0$ and $u > 0$,

$$\mathbb{E}[V_t | \mathcal{F}_{t_0}] = V_0 e^{-\kappa t} + \bar{V}(1 - e^{-\kappa t}) + \int_0^{t_0} h(t, s) dX_s + \xi_1 \int_{t_0}^t h(t, s) ds \quad (21)$$

and

$$\text{Cov}[X_t^{(h)}, X_{t+u}^{(h)} | \mathcal{F}_{t_0}] = \xi_2 \int_{t_0}^t h(t, s) h(t+u, s) ds - \xi_1^2 \left(\int_{t_0}^t h(t, s) ds \right) \left(\int_{t_0}^{t+u} h(t+u, s) ds \right).$$

2.3 Average forward volatility

After constructing the instantaneous variance model with roughness and jumps, we now proceed to giving a convenient structure for the forward variance curve, i.e.,

$$\tilde{V}_t(u) := \mathbb{E}[V_{t+u} | \mathcal{F}_t], \quad u > 0, t \geq 0, \quad (22)$$

which in light of (21) admits the following stochastic integral representation,

$$\tilde{V}_t(u) = V_0 e^{-\kappa(t+u)} + \bar{V}(1 - e^{-\kappa(t+u)}) + X_t^{(H_u)} + \xi_1 \int_t^{t+u} H_u(t, s) ds, \quad (23)$$

where $X^{(H_u)}$ is associated with the u -shifted kernel

$$H_u(t, s) := h(t+u, s), \quad u > 0. \quad (24)$$

Apart from the contemporaneous instantaneous variance, frictions in the forward variance curve also result from a new fractional Lévy process $X^{(H_u)}$ containing additional information over the entire variance history. In consequence, with a general kernel h the Markov property of $\tilde{V}(u)$ is completely lost. If one prefers to view $t+u > t$ as being time-independent, then (23) really gives a martingale dynamics for the forward variance curve over $[0, t+u]$, which is similar to the martingale framework developed in [Horvath, 2020, Sect. 3] [14]. However, we intentionally refrain from operating on such a framework as it is primarily beneficial from a simulation-based viewpoint. It is also worth emphasizing that, since $\lim_{s \nearrow t} H_u(t, s) = h(t+u, t) = O(1)$, $\forall t, u > 0$, the modified process $X^{(H_u)}$ deprives the sample paths of $\tilde{V}(u)$ of any degree of roughness.

Under continuous monitoring over a fixed window $\Theta > 0$, the average forward volatility process is identified as the square root of the Θ -running average of the forward variance process

$$I_t^*(\Theta) := \sqrt{\frac{1}{\Theta} \int_0^\Theta \tilde{V}_t(u) du}, \quad t \geq 0.$$

In the case of the VIX index, for instance, $\Theta = 30/365 = 6/73$ year. This continuous monitoring formula can be incommodious in that it requires integration of the kernel H_u in u over a compact interval, hence resulting in significant complication. For this reason, we use the fact that H_u and the integrated kernel $\int_0^u H_w dw/u$ are both continuously differentiable and bounded functions with identical tail behaviors for every $u \in (0, \Theta]$ and propose the following approximation of $I^*(\Theta)$

$$I_t(\Delta) = \sqrt{\tilde{V}_t(\Delta)}, \quad t \geq 0, \quad (25)$$

for some adjusted window $\Delta \in (0, \Theta]$ which depends on the shape of h and should most likely be treated as an additional parameter⁴. In other words, by (25) we attempt to approximate $I^*(\Theta)$ as the Δ -forward volatility. It is clear that neither $I^*(\Theta)$ nor $I(\Delta)$ can possess rough sample paths and from now on we will refer to $I(\Delta)$ as the (adjusted) average forward volatility, taking it as a replacement of $I^*(\Theta)$. At this point, a comfortable integral formula for the conditional characteristic function of the (adjusted) average forward variance is readily available, which we formulate as the following proposition.

Proposition 2. *In the setting with (6) and (25), we have for any $0 \leq t_0 < t \leq T$ and $\Delta \in (0, \Theta]$ that*

$$\begin{aligned} \phi_{t_0, t}(l; \Delta) &:= \mathbb{E}[e^{ilI_t^2(\Delta)} | \mathcal{F}_{t_0}] \\ &= \exp\left(il\left(I_{t_0}^2(t - t_0 + \Delta) - \xi_1 \int_{t_0}^t H_\Delta(t, s) ds\right) + \int_{t_0}^t \log \phi_{X_1}(lH_\Delta(t, s)) ds\right), \quad l \in \mathbb{R}, \end{aligned} \quad (26)$$

with the modified kernel H_Δ specified in (24).

With Proposition 2 one can deduce pricing-hedging formulae for derivatives contracts written on the average forward variance, e.g., the squared VIX index, which will be explained in detail in the next section. Most importantly, although it is not possible to derive a similar formula for the characteristic function of the average forward volatility, we will demonstrate how this difficulty may be overcome for volatility derivatives by way of power-type extensions. Moreover, by forcing $\Delta \searrow 0$ (26) is nothing but the conditional characteristic function for the instantaneous variance, i.e., $\mathbb{E}[e^{ilV_t} | \mathcal{F}_{t_0}]$, $l \in \mathbb{R}$.

Since $I^2(u)$ is an adapted process for every $u > 0$ we notice that $I_{t_0}^2(t - t_0 + \Delta)$ in (26) is measurable with respect to \mathcal{F}_{t_0} , and is recoverable from an entire realized sample path of $I(\Delta)$ up to t_0 . Also, computation of the first Riemann integral is fairly straightforward, and one gets the following explicit expression⁵ under the type-I kernel,

$$\int_{t_0}^t H_\Delta(t, s) ds = \frac{\Gamma(d, \kappa \Delta) - \Gamma(d, \kappa(t - t_0 + \Delta))}{\kappa^d \Gamma(d)} \quad (27)$$

and similarly, under the type-II kernel, it is

$$\int_{t_0}^t H_\Delta(t, s) ds = \frac{e^{-\kappa \Delta} (\Gamma(d) - \Gamma(d, -\kappa \Delta)) - e^{-\kappa(t - t_0 + \Delta)} (\Gamma(d) - \Gamma(d, -\kappa(t - t_0 + \Delta)))}{(-\kappa)^d \Gamma(d)}. \quad (28)$$

On the other hand, to evaluate the second Riemann integral in (26) analytically is far from an easy task, even with the specialization that X is a tempered stable subordinator having the characteristic exponent (5). In this case, for h being the kernel of either type I or type II, no explicit expression exists for such an integral, the computation of which has to resort to numerical methods such as the Gauss quadrature rule ([Golub and Welsch, 1969] [13]). The reason behind this problem is simple: the type-I and type-II kernels are both formed

⁴The determination rule of Δ will be further discussed in Section 5.1.

⁵The expression under the type-III kernel is specifically put into Corollary 1 and one is referred to its proof in Section 8.3.

by multiplying power and exponential functions but no elementary substitution works for integrals of the form $\int (1 - e^{-\kappa s} s^{d-1})^c ds$, for $d > 1/2$, $\kappa > 0$ and $c \in (0, 1)$. At this point, it is no surprise that with the type-III kernel an explicit formula is accessible due to the aforementioned power-exponential multiplication reflected in the time-invariant threshold $\tau > 0$, while by its piecewise nature neither path roughness nor the mean-reverting property of the instantaneous variance is sacrificed. This gives rise to the following important corollary.

Corollary 1. *Let h be the type-III kernel in (14), with $d \in (1/2, 1)$, and let X_1 have the characteristic exponent (5). Then we have*

$$\begin{aligned} \phi_{t_0, t}(l; \Delta) = \exp \Big(& i l I_{t_0}^2(t - t_0 + \Delta) \\ & + \begin{cases} Y_-(s)|_{s=\Delta}^{t-t_0+\Delta} & \text{if } \tau > t - t_0 + \Delta, \\ Y_-(s)|_{s=\Delta}^{\max\{\tau, \Delta\}} + Y_+(s)|_{s=\max\{\tau, \Delta\}}^{t-t_0+\Delta} & \text{if } \tau \leq t - t_0 + \Delta \end{cases} \Big), \quad l \in \mathbb{R}, \end{aligned} \quad (29)$$

where for $s \in [\Delta, t - t_0 + \Delta]$

$$Y_+(s) := \frac{i l a \theta \Gamma(1-c) e^{-\kappa s}}{\kappa b^{1-c}} + a \Gamma(-c) \left(\frac{e^{\kappa s} (b - i l \theta e^{-\kappa s})^{c+1}}{i l c \kappa \theta} {}_2F_1\left(1, 1; 1-c; \frac{b e^{\kappa s}}{i l \theta}\right) - b^c s \right) \quad (30)$$

and

$$\begin{aligned} Y_-(s) := & \frac{i l a \Gamma(1-c) s}{b^{1-c}} \left(\frac{d \tau^{d-1} - s^{d-1}}{\Gamma(d+1)} - \theta e^{-\kappa \tau} \right) + a \Gamma(-c) s \left(\left(b - i l \theta e^{-\kappa \tau} + \frac{i l \tau^{d-1}}{\Gamma(d)} \right)^c \right. \\ & \times \left. {}_2F_1\left(-c, \frac{1}{d-1}, \frac{d}{d-1}; \frac{i l s^{d-1}}{i l \tau^{d-1} + (b - i l \theta e^{-\kappa \tau}) \Gamma(d)}\right) - b^c \right). \end{aligned} \quad (31)$$

As a remark, by forcing $\tau \rightarrow \infty$ one obtains the characteristic function in the absence of mean reversion, with $\kappa \searrow 0$ equivalently, and this is acceptable when specifically dealing with derivatives with short maturities. On the contrary, taking $\tau \searrow 0$ corresponds to $d \nearrow 1$ which removes roughness. These two extremal cases⁶, in which the $Y_-(s)$ and $Y_+(s)$ terms in (31) vanish respectively, underlie contrast analysis for our implementation.

3 Simulation techniques

Despite non-stationarity in general, using (6) we can still simulate the sample paths of the instantaneous variance process. To do this, we discretize the generic interval $[0, T]$ by means of the uniform partition

$$\mathbf{T}_M := \left\{ \frac{nT}{M} \right\}_{n=0}^M, \quad M \in \mathbb{N}_{++}, \quad M \gg 1. \quad (32)$$

⁶Noticeably, the latter extremal case is only achievable when θ is strictly larger than the lower bound in (16), and not from (18), where θ vanishes in the limit.

Then, using the Gauss quadrature rule and the Lévy properties of X , we have the following estimator of (6) on \mathbf{T}_M which replaces the Volterra-type stochastic integral with a finite random sum.

$$\check{V}_{nT/M} = V_0 e^{-\kappa nT/M} + \bar{V}(1 - e^{-\kappa nT/M}) + \sum_{k=0}^{n-1} h\left(\frac{nT}{M}, \frac{kT}{M}\right) \check{X}_k, \quad n \geq 1, \quad (33)$$

where \check{X}_k 's are i.i.d. random variables with characteristic function $\phi_{\check{X}_k}(l) := \mathbb{E}[e^{il\check{X}_k}] = (\phi_{X_1}(l))^{T/M}$, for $l \in \mathbb{R}$. If the kernel is stationary, $h(nT/M, kT/M) = h((n-k)T/M)$. The next proposition describes the convergence rate of the discretized process \check{V} towards V over $(0, T]$ (with trivial equivalence at time 0).

Proposition 3. *Under \mathbf{T}_M , for any fixed $t \in (0, T]$, there exists $n \in \mathbb{N} \cap [1, M]$ such that the estimator $\check{V}_{nT/M}$ is conditionally asymptotically unbiased towards V_t and*

$$\mathbb{E}[(\check{V}_{nT/M} - V_t)^2] = O(M^{-1}), \quad \text{as } M \rightarrow \infty.$$

Note that the convergence rate is untrammelled by the fraction index d of h , which applies to the three types of kernels discussed. Nonetheless, the above L^2 -convergence fails in the limit as $d \searrow 1/2$. In a similar fashion, we can use (25) to simulate the sample paths of the average forward variance $I^2(\Delta)$ for a given $\Delta > 0$, by using the estimator

$$\begin{aligned} \check{I}_{nT/M}^2(\Delta) &= V_0 e^{-\kappa(nT/M+\Delta)} + \bar{V}(1 - e^{-\kappa(nT/M+\Delta)}) + \sum_{k=0}^{n-1} H_\Delta\left(\frac{nT}{M}, \frac{kT}{M}\right) \check{X}_k \\ &\quad + \int_{nT/M}^{nT/M+\Delta} H_\Delta\left(\frac{nT}{M}, s\right) ds, \quad n \in \mathbb{N} \cap [1, M], \end{aligned} \quad (34)$$

to which the L^2 -convergence criterion in Proposition 3 also applies, and where there is no need to discretize the last deterministic integral which can be evaluated explicitly in many cases; see, e.g., (25), (26) and Corollary 1 as well.

We illustrate (33) by considering X to be a gamma process and an inverse Gaussian process, both belonging to the class of tempered stable processes; recall (5). The reason is that in these two cases the cumulative distribution function of \check{X}_1 can be expressed in closed form which facilitates the use of inverse transform sampling. In light of the previous discussion based on Figure 1 we focus on the type-I kernel (9) and use the parameters $\kappa = 1$ and $V_0 = \bar{V} = 0.5$, the adjusted window $\Delta = 6/73$, as well as $M = 1000$ quadratures. In Figure 2⁷ we plot realized sample paths of V over the unit time interval for both $d = 0.6$ and $d = 1.1$.

We can see that the simulated paths under $d = 0.6$ are much rougher than those under $d = 1.1$. In fact, from Proposition 1 we know that in the former case the sample paths of V are purely discontinuous with probability 1, whereas in the latter case they are continuous. These illustrations are to show that the proposed rough stochastic volatility model

⁷The values of a and b are chosen for the mean and variance of X_1 in the gamma case to match those in the inverse Gaussian case, which are $1/5$ and $1/2500$, respectively.

with jumps can be simulated effectively, in spite of increment non-stationarity, thus implying potential applications to simulation-based pricing methods, which are however not our concentration in the present paper.

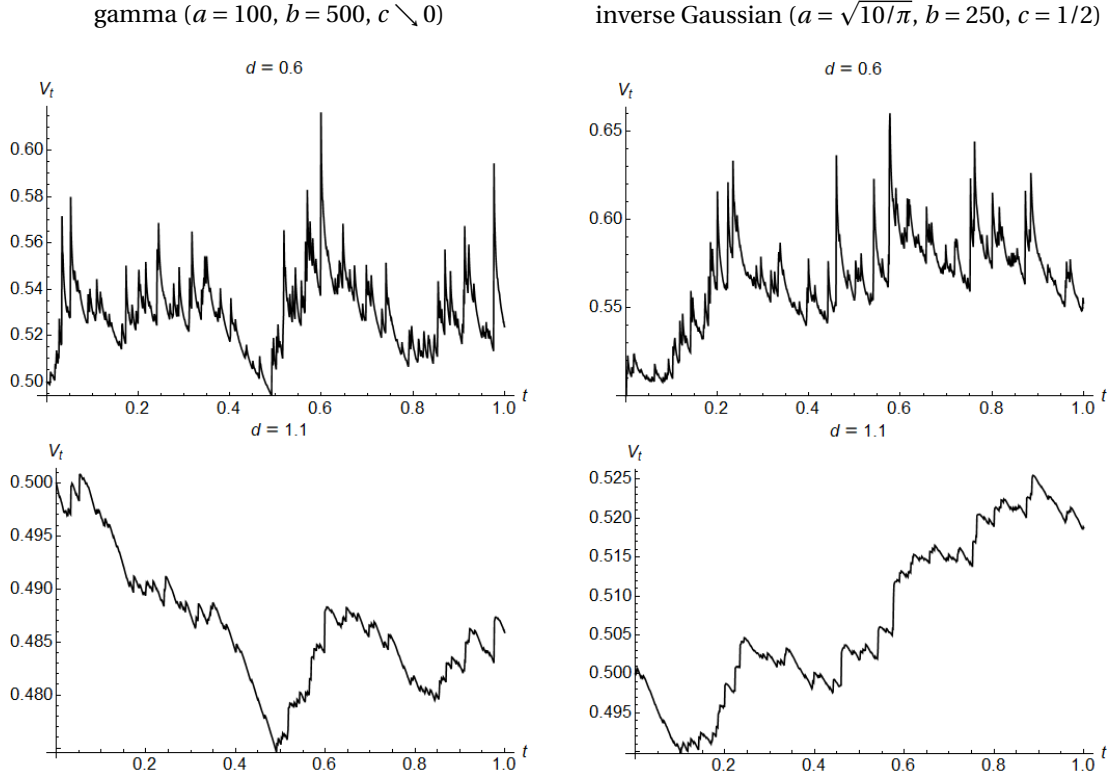


Figure 2: Simulated sample paths of V

4 Power-type derivatives

In this section we present the main pricing-hedging formulae for European-style derivatives written on the adjusted average forward volatility. The setting of Section 2.2, esp. the representation (6), is adopted throughout, and a fixed maturity date $T > 0$ is assumed.

4.1 Power swaps

We begin with swaps written on the average forward volatility. The payoff of a power swap to its investor is at T

$$S_T^{(p)} = I_T^p(\Delta), \quad (35)$$

where $p \geq 0$ is a predetermined power coefficient. Here we have discarded the notional amount for simplicity as it is merely a positive scaling factor. Of course, the extremal case

$p = 0$ corresponds to a fixed cash payment of 1 dollar, while by choosing $p = 1$ and $p = 2$, one obtains the standard volatility swap and the standard variance swap, respectively.

Convention is that, at inception of trading, the price of the swap is set to achieve a zero fair value, and so the price of the swap at a given time point t_0 before maturity can be simply computed as the expected value of $I_T^p(\Delta)$ conditional on \mathcal{F}_{t_0} , i.e., as

$$S_{t_0}^{(p)} = \mathbb{E}[I_T^p(\Delta) | \mathcal{F}_{t_0}],$$

and is treatable as a potentially fractional moment of $I_T^2(\Delta)$, which is naturally connected to the so-called “fractional calculus”.

Proposition 4. *At time $t_0 \in [0, T)$, the price of the power volatility swap with payoff (35) satisfies the quasi-recurrence relation⁸*

$$\begin{aligned} S_{t_0}^{(p)} &= (-i)^{p/2} \phi_{t_0, T}^{(p/2)}(0; \Delta), \quad p \in 2\mathbb{N}, \\ \rightsquigarrow S_{t_0}^{(p)} &= \sec \frac{\pi(p/2 - \lfloor p/2 \rfloor)}{2} \frac{p/2 - \lfloor p/2 \rfloor}{\Gamma(1 - p/2 + \lfloor p/2 \rfloor)} \\ &\quad \times \int_0^\infty \operatorname{Re} \left[\frac{S_{t_0}^{(2\lfloor p/2 \rfloor)} - (-i)^{\lfloor p/2 \rfloor} \phi_{t_0, T}^{(\lfloor p/2 \rfloor)}(l; \Delta)}{l^{p/2 - \lfloor p/2 \rfloor + 1}} \right] dl, \quad p \notin 2\mathbb{N}, \end{aligned} \quad (36)$$

provided that $\mathbb{E}[I_T^p(\Delta)] < \infty$.

Thanks to the exponential structure (26) the convergence of (36) can be directly linked to the smoothness of the characteristic function of X_1 . Comprehensibly, it is never exorbitant to demand that $\phi_{t_0, T}(\cdot; \Delta) \in \mathcal{C}^{\lfloor p/2 \rfloor + 1}(\mathbb{R})$, which condition remains valid for a wide class of square-integrable Lévy processes X . For instance, for X a tempered stable process, its characteristic function (5) immediately renders $\phi_{t_0, T}(\cdot; \Delta) \in \mathcal{C}^\infty(\mathbb{R})$ so that Proposition 4 is automatically applicable for all values of $p \geq 0$. Implementation of (36) is also quite straightforward, the specializations in Corollary (1) notwithstanding, by means of the Gauss quadrature rule for numerical integration and finite-difference approximations for differentiation of integer orders; for example, given the required degree of smoothness, a central approximation reads for $\epsilon > 0$ small

$$\phi_{t_0, T}^{(\lfloor p/2 \rfloor)}(0; \Delta) = \sum_{n=0}^{\lfloor p/2 \rfloor} \binom{\lfloor p/2 \rfloor}{n} (-1)^n \phi_{t_0, T} \left(\left(\frac{\lfloor p/2 \rfloor}{2} - 1 \right) \epsilon; \Delta \right) + O(\epsilon^2).$$

In particular, by taking $p = 1$ in (36) the pricing formula for the standard volatility swap reads

$$S_{t_0}^{(1)} = \frac{1}{\sqrt{2\pi}} \int_0^\infty \operatorname{Re} \left[\frac{1 - \phi_{t_0, T}(l; \Delta)}{\sqrt{l^3}} \right] dl, \quad (37)$$

whilst that for the corresponding variance swap is none but the \mathcal{F}_{t_0} -conditional mean of $I_T^2(\Delta)$ and we recall (22) and (25).

⁸For simplicity we use $\phi_{t_0, T}^{(\omega)}(l; \Delta) \equiv \partial^\omega \phi_{t_0, T}(l; \Delta) / \partial l^\omega$ to denote the ω th derivative of $\phi_{t_0, T}(l; \Delta)$ with respect to $l \in \mathbb{R}$, for $\omega \geq 0$.

As we are amidst a non-Markovian setting, it is quixotic to construct a hedge for these power volatility swaps based on the contemporaneous average forward variance $I_{t_0}^2(\Delta)$. In light of the presentation of the characteristic function (26), to hedge such a swap one should need at least the forward variance with a prolonged window by the time to maturity, whose variable nature with regard to the current date t_0 gives rise to a dynamic hedging strategy. In other words, a hedging strategy designated for the time period $[t_0, T]$ will require the entire forward variance curve $\{\tilde{V}_{t_0}(u) : u \in (\Delta, T - t_0 + \Delta]\}$. The good news is that perfect hedging is possible using only the forward variance curve, with no additional sources of risk involved in the swap, as the next corollary explains. To that end we first define the time-indexed differential operator

$$\Delta_t := \frac{\partial}{\partial I_{t_0}^2(t - t_0 + \Delta)}, \quad t \in [t_0, T],$$

for a fixed $t_0 \in [0, T]$.

Corollary 2. *In the setting of Proposition 4 we have⁹*

$$\begin{aligned} \Delta_T(S_{t_0}^{(p)}) &= \frac{p(-i)^{p/2-1} \phi_{t_0, T}^{(p/2-1)}(0; \Delta)}{2} = \frac{p S_{t_0}^{(p-2)}}{2}, \quad p \in 2\mathbb{N}, \\ \rightsquigarrow \Delta_T(S_{t_0}^{(p)}) &= \sec \frac{\pi(p/2 - \lfloor p/2 \rfloor)}{2} \frac{p/2 - \lfloor p/2 \rfloor}{\Gamma(1 - p/2 + \lfloor p/2 \rfloor)} \int_0^\infty \operatorname{Re} \left[\frac{1}{l^{p/2 - \lfloor p/2 \rfloor + 1}} \left(\Delta_T(S_{t_0}^{(2\lfloor p/2 \rfloor)}) \right. \right. \\ &\quad \left. \left. - (-i)^{\lfloor p/2 \rfloor - 1} \left(l \phi_{t_0, T}^{(\lfloor p/2 \rfloor)}(l; \Delta) + \left\lfloor \frac{p}{2} \right\rfloor \phi_{t_0, T}^{(\lfloor p/2 \rfloor - 1)}(l; \Delta) \right) \right) \right] dl, \quad p \notin 2\mathbb{N}. \end{aligned} \quad (38)$$

The first equation in (38) signifies that if $p/2$ is an integer, then the size of the hedge is equal to the spot price of another power variance swap, with the decremented power $p/2 - 1$. Again, after taking $p = 1$ in the second equation, we find the hedge for the standard volatility swap as

$$\Delta_T(S_{t_0}^{(1)}) = \frac{1}{\sqrt{2\pi}} \int_0^\infty \operatorname{Re} \left[\frac{\phi_{t_0, T}(l; \Delta)}{\sqrt{l}} \right] dl.$$

Obviously, for the corresponding variance swap, the hedge is exactly $I_{t_0}^2(T - t_0 + \Delta)$, with $\Delta_T(S_{t_0}^{(2)}) = 1$.

Moreover, we stress that the convergence of (38) does not rely on integrability of the characteristic function, namely $\phi_{t_0, T}(\cdot; \Delta) \in L^1(\mathbb{R})$. In fact, although this condition is considerably benign and realistic, it is only sufficient but not necessary for the results to hold. The only assumption we have made in this regard is that X_1 is a continuous random variable, stemming from the non-atomic Lévy measure ν .

4.2 Asymmetric power options

As mentioned since the introduction, our study for asymmetric power options is motivated by the average forward volatility being the square root of the average forward variance. In other words, an option written on the average forward volatility can be effectively

⁹ Although the notation $\phi_{t_0, T}^{(-1)}(\cdot; \Delta)$ can be well understood as an antiderivative, it does not matter here due to multiplication by 0.

treated as a power-type option on the average forward variance, with power exactly equal to $1/2$. For convenience and generality we still conduct our analysis subject to a positive power coefficient.

Let us consider a European-style put option contract on the average forward volatility $I_T(\Delta)$, having the terminal payoff

$$P_T^{(p_1, p_2, (a))} = (K^{p_2} - I_T^{p_1}(\Delta))^+, \quad (39)$$

where $K > 0$ is the volatility strike and $p_1, p_2 \geq 0$ are two predetermined power coefficients. We refer to this type as being asymmetric since the power imposed on the strike can differ from that on the average forward volatility. The payoff structure (39) grants the option investor a leveraged view on the average forward volatility. Since $I_T(\Delta)$ takes values within the unit interval under normal conditions, $p_1 > 1$ actually reduces the option investor's risk exposure, other things equal, while $0 \leq p_1 < 1$ expands it, which is the exact opposite of the case of equity options (see [Xia, 2019, pp. 119] [39]). Obviously, for any fixed $p_2 \geq 0$, $P_T^{(1, p_2, (a))}$ corresponds to the terminal payoff of the standard volatility put option, while $P_T^{(1, p_2, (a))}$ represents that of a standard put option on the average forward variance. Moreover, in the case of a call option, we have

$$C_T^{(p_1, p_2, (a))} = (I_T^{p_1}(\Delta) - K^{p_2})^+. \quad (40)$$

The following proposition is given for arbitrary-time pricing of the asymmetric power option.

Proposition 5. *The price of the asymmetric power put option with terminal payoff (39) at time $t_0 \in [0, T)$ is given by*

$$P_{t_0}^{(p_1, p_2, (a))} = \frac{K^{p_2}}{2} - \frac{1}{\pi} \int_0^\infty \operatorname{Re} \left[\left(K^{p_2} e^{-iK^{2p_2/p_1} l} + \frac{\Gamma(p_1/2 + 1) - \Gamma(p_1/2 + 1, iK^{2p_2/p_1} l)}{(il)^{p_1/2}} \right) \times \frac{\phi_{t_0, T}(l; \Delta)}{il} \right] dl. \quad (41)$$

The price of the asymmetric power call option with terminal payoff (40) at time $t_0 \in [0, T)$ is given by

$$C_{t_0}^{(p_1, p_2, (a))} = P_{t_0}^{(p_1, p_2, (a))} - K^{p_2} + S_{t_0}^{(p_1)}, \quad (42)$$

where $S_{t_0}^{(p_1)}$ is the contemporaneous price of a power swap on $I_T(\Delta)$ specified in Proposition 4.

By taking $p_1 = p_2 = 1$ one has the pricing formulae for the standard volatility options. In particular,

$$P_{t_0}^{(1, 1, (a))} = \frac{K}{2} - \frac{1}{\pi} \int_0^\infty \operatorname{Re} \left[\left(K e^{-iK^2 l} + \frac{\sqrt{\pi}/2 - \Gamma(3/2, iK^2 l)}{\sqrt{il}} \right) \frac{\phi_{t_0, T}(l; \Delta)}{il} \right] dl. \quad (43)$$

and, recalling (37),

$$C_{t_0}^{(1, 1, (a))} = \frac{1}{\pi} \int_0^\infty \operatorname{Re} \left[\sqrt{\frac{\pi}{2l^3}} - \left(K e^{-iK^2 l} + \frac{i\sqrt{\pi}/2 - \Gamma(3/2, iK^2 l)}{\sqrt{il}} \right) \frac{\phi_{t_0, T}(l; \Delta)}{il} \right] dl - \frac{K}{2}. \quad (44)$$

On the other hand, for the standard put option on the average forward variance with $p_1 = 2$, there is a significant reduction,

$$P_{t_0}^{(2,1,(a))} = \frac{K}{2} - \frac{1}{\pi} \int_0^\infty \operatorname{Re} \left[\frac{(e^{-iKl} - 1)\phi_{t_0,T}(l; \Delta)}{l^2} \right] dl.$$

The formulae (43) and (44) for the standard volatility options can be implemented with high efficiency provided that the conditional characteristic function takes the form of (26) and facilitate calibration of the model on standard option prices.

Hedging of the asymmetric power options resembles that of the corresponding power swap, with complete reliance on the forward variance curve. For the following we adopt the differential operator Δ_t for $t \in [t_0, T]$.

Corollary 3. *In the setting of Proposition 5, hedges can be constructed as*

$$\begin{aligned} \Delta_T(P_{t_0}^{(p_1, p_2, (a))}) = & -\frac{1}{\pi} \int_0^\infty \operatorname{Re} \left[\left(K^{p_2} e^{-iK^2 p_2 / p_1 l} + \frac{\Gamma(p_1/2 + 1) - \Gamma(p_1/2 + 1, iK^2 p_2 / p_1 l)}{(il)^{p_1/2}} \right) \right. \\ & \left. \times \phi_{t_0,T}(l; \Delta) \right] dl \end{aligned} \quad (45)$$

and

$$\Delta_T(C_{t_0}^{(p_1, p_2, (a))}) = \Delta_T(P_{t_0}^{(p_1, p_2, (a))}) + \Delta_T(S_{t_0}^{(p_1)}), \quad (46)$$

where $\Delta_T(S_{t_0}^{(p_1)})$ is as specified in Corollary 2.

Once again, with the choice $p_1 = p_2 = 1$, the standard volatility options can be hedged in terms of

$$\Delta_T(P_{t_0}^{(1,1,(a))}) = -\frac{1}{\pi} \int_0^\infty \operatorname{Re} \left[\left(K e^{-iK^2 l} + \frac{\sqrt{\pi}/2 - \Gamma(3/2, iK^2 l)}{\sqrt{il}} \right) \phi_{t_0,T}(l; \Delta) \right] dl$$

and

$$\Delta_T(C_{t_0}^{(1,1,(a))}) = \frac{1}{\pi} \int_0^\infty \operatorname{Re} \left[\left(\frac{i\sqrt{\pi}/2 - \Gamma(3/2, iK^2 l)}{\sqrt{il}} - K e^{-iK^2 l} \right) \phi_{t_0,T}(l; \Delta) \right] dl.$$

As always, one should never neglect the fact that hedging with the underlying average forward variance $I^2(\Delta)$ is possible if V is a conventional Ornstein-Uhlenbeck process with $h(t, s) = e^{\kappa(t-s)}$. In this respect, Corollary 2 and Corollary 3 provide alternative hedging strategies based on a prolonged window, which remain valid with or without rough volatility. On the other hand, these newfound hedges, albeit nonexclusive, are certainly very convenient since the investor only needs to look at one single forward variance, instead of the entire curve, at any given date before maturity.

4.3 Symmetric power options

As in the case of equity options, the volatility option investor's risk exposure can also be adjusted by directly forcing a mutual power effect on the standard option payoff (similar to [Raible, 2000, Sect. 3.4] [28] and [Xia, 2019, pp. 120] [39]). This way of generalization

understandably does not build any useful connection between options on the average forward volatility and the corresponding forward variance and is hence considered less important from the viewpoint of this paper's motivation. Nonetheless, for the sake of completeness and our interest we still provide a comprehensive analysis of the pricing-hedging methods for such so-called "symmetric power options".

In this connection let a European-style put option contract on $I_T(\Delta)$ have the following terminal payoff,

$$P_T^{(p,(s))} = ((K - I_T(\Delta))^+)^p, \quad (47)$$

where $K > 0$ and $p \geq 0$. In this structure both the strike price and the average forward volatility undergo the same power impact, and with binomial expansion we can rewrite

$$P_T^{(p,(s))} = \sum_{k=0}^{\infty} \binom{p}{k} (-1)^k K^{p-k} I_T^k(\Delta) \mathbb{1}_{\{I_T(\Delta) < K\}} = \sum_{k=0}^{\infty} \binom{p}{k} (-1)^k K^{p-k} S_T^{(k)} \mathbb{1}_{\{I_T(\Delta) < K\}}, \quad (48)$$

which shows that, conditional on $\{I_T(\Delta) < K\}$, the symmetric put power option can be looked upon as a weighted sum of power volatility swaps, each associated with an integer power coefficient in \mathbb{N} , which at $k = 0$ is merely a cash payment of K^p . Clearly, (48) is a finite sum if and only if $p \in \mathbb{N}$.

Besides, we observe that the plots of the payoff functions $P_T^{(p,p,(a))}$ and $P_T^{(p,(s))}$ against $I_T(\Delta)$ are symmetric with respect to the line segment joining the points $(0, K^p)$ and $(K, 0)$ over the interval $[0, K]$. For $0 \leq p < 1$, the symmetric power option provides a convex transformation of the standard option payoff whereas its asymmetric power counterpart provides a concave one; for $p > 1$ one has a reversed relation (see Figure 3 below). Therefore, the two types of power put options can be utilized to complement each other in terms of severity of risk adjustment when either deeply in-the-money or closed to at-the-money. However, such effect holds exclusively for put options.

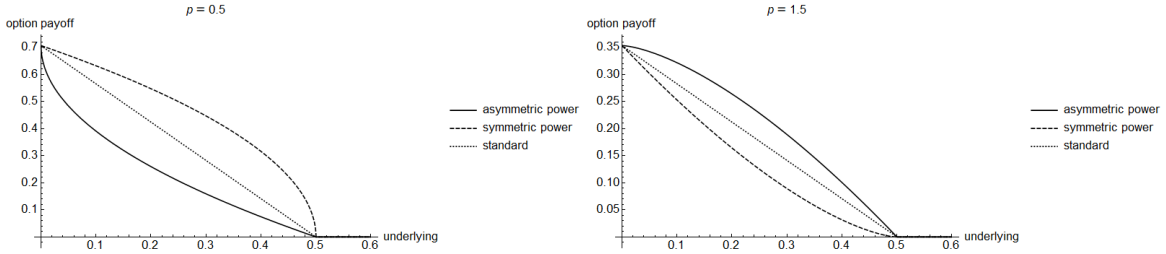


Figure 3: Comparison of leverage effects of power put options

As we write the terminal payoff

$$\begin{aligned} C_T^{(p,(s))} &= ((I_T(\Delta) - K)^+)^p \\ &= \begin{cases} \sum_{k=0}^p \binom{p}{k} (-K)^k S_T^{(p-k)} \mathbb{1}_{\{I_T(\Delta) > K\}}, & p \in \mathbb{N}, \\ \left(\sum_{k=0}^{\lfloor p \rfloor} \binom{p}{k} (-K)^k S_T^{(p-k)} + \sum_{k=\lfloor p \rfloor+1}^{\infty} \binom{p}{k} (-K)^k I_T^{p-k}(\Delta) \right) \mathbb{1}_{\{I_T(\Delta) > K\}}, & p \notin \mathbb{N}, \end{cases} \end{aligned} \quad (49)$$

a similar symmetric power call option can be decomposed into exactly $\lfloor p \rfloor$ weighted power volatility swaps incremented by an infinite sequence of power-type derivatives on the reciprocal average forward volatility $I_T^{-1}(\Delta)$ conditioned to stay below $1/K$, which vanishes if and only if p is an integer. Also, note that in this case the payoff functions $C_T^{(p,p,(a))}$ and $C_T^{(p,(s))}$ are both strictly concave resp. convex in $I_T(\Delta)$ for $0 \leq p < 1$ resp. $p > 1$ over $[K, \infty)$, with $\lim_{x \rightarrow \infty} (x^p - K^p)^+ / ((x - K)^+)^p = 1$.

Based on the two decompositions (48) and (49), the next proposition gives the pricing formulae for these symmetric power options in terms of infinite series.

Proposition 6. *The price of the symmetric power put option with terminal payoff (47) at time $t_0 \in [0, T)$ is given by*

$$P_{t_0}^{(p,(s))} = \frac{1}{\pi} \sum_{k=0}^{\infty} \binom{p}{k} (-1)^k K^{p-k} \int_0^{\infty} \operatorname{Re} \left[\frac{(\Gamma(k/2 + 1) - \Gamma(k/2 + 1, iK^2 l)) \phi_{t_0, T}(l; \Delta)}{(il)^{k/2+1}} \right] dl, \quad (50)$$

while that of the similar symmetric power call option with (49) is

$$C_{t_0}^{p,(s)} = \sum_{k=0}^{\lfloor p \rfloor} \binom{p}{k} (-K)^k \left(S_{t_0}^{(p-k)} - \frac{1}{\pi} \int_0^{\infty} \operatorname{Re} \left[\frac{(\Gamma((p-k)/2 + 1) - \Gamma((p-k)/2 + 1, iK^2 l)) \phi_{t_0, T}(l; \Delta)}{(il)^{(p-k)/2+1}} \right] dl \right) + \Sigma_{t_0}^{(p)}, \quad (51)$$

where $S_{t_0}^{(p-k)}$'s, for $0 \leq k \leq p$, are the contemporaneous power swap prices as specified in Proposition 4 and

$$\Sigma_{t_0}^{(p)} = \begin{cases} 0, & \text{if } p \in \mathbb{N}, \\ \frac{1}{\pi} \sum_{k=\lfloor p \rfloor+1}^{\infty} \binom{p}{k} (-K)^k \int_0^{\infty} \operatorname{Re} \left[\frac{\Gamma(1 - (k-p)/2, iK^2 l) \phi_{t_0, T}(l; \Delta)}{(il)^{1-(k-p)/2}} \right] dl, & \text{if } p \notin \mathbb{N}. \end{cases}$$

Hedges of these symmetric power options using $I_{t_0}^2(T - t_0 + \Delta)$ also come in similar forms, which yield the next result.

Corollary 4. *Assume the setting of Proposition 6. Then we have*

$$\Delta_T(P_{t_0}^{(p,(s))}) = \frac{1}{\pi} \sum_{k=0}^{\infty} \binom{p}{k} (-1)^k K^{p-k} \int_0^{\infty} \operatorname{Re} \left[\frac{(\Gamma(k/2 + 1) - \Gamma(k/2 + 1, iK^2 l)) \phi_{t_0, T}(l; \Delta)}{(il)^{k/2}} \right] dl,$$

and

$$\begin{aligned} \Delta_T(C_{t_0}^{p,(s)}) &= \Delta_T(\Sigma_{t_0}^{(p)}) + \sum_{k=0}^{\lfloor p \rfloor} \binom{p}{k} (-K)^k \left(\Delta_T(S_{t_0}^{(p-k)}) \right. \\ &\quad \left. - \frac{1}{\pi} \int_0^{\infty} \operatorname{Re} \left[\frac{(\Gamma((p-k)/2 + 1) - \Gamma((p-k)/2 + 1, iK^2 l)) \phi_{t_0, T}(l; \Delta)}{(il)^{(p-k)/2}} \right] dl \right), \end{aligned}$$

where $\Delta_T(S_{t_0}^{(p-k)})$'s, for $0 \leq k \leq p$, are the contemporaneous power swap hedges as specified in Corollary 2 and

$$\Delta_T(\Sigma_{t_0}^{(p)}) = \begin{cases} 0, & \text{if } p \in \mathbb{N}, \\ \frac{1}{\pi} \sum_{k=\lfloor p \rfloor + 1}^{\infty} \binom{p}{k} (-K)^k \int_0^{\infty} \operatorname{Re} \left[\frac{\Gamma(1 - (k - p)/2, iK^2 l) \phi_{t_0, T}(l; \Delta)}{(il)^{(p-k)/2}} \right] dl, & \text{if } p \notin \mathbb{N}. \end{cases}$$

5 An empirical study

For this empirical study we illustrate the performance of our model framework established in Section 2 as well as the pricing-hedging formulae presented in Section 4. Allowing for overall efficiency, we focus on the closed-form characteristic function presented in Corollary 1, specializing h according to (18) and taking X to belong to the class of tempered stable subordinators.

5.1 Data and preparation

Our data set consists of standard VIX option prices quoted on June 1, 2016, in the unit of US\$100. On this date, the VIX index closed at $I_0(\Delta) = 0.1424$. We extract from the data set 38 call options for our calibration purpose¹⁰. These are four different maturities $T = 7, 28, 112, 168$ days and the strike price K goes from 0.1 to as high as 0.7, and $t_0 = 0$ is set for simplicity.

For the VIX index we fix $\Theta = 6/73$ year. In order to apply Proposition 2 properly, several ingredients are to be specified. First and foremost, we need to agree on how to compute the adjusted window Δ . As aforementioned, we can of course take it as a parameter and put it into our calibration scheme. However, since in this case by the definition of the type-III kernel both $H_{\Delta}(T - \cdot)$ and $\int_0^{\Theta} H_u(T - \cdot) du / \Theta$ are stationary, strictly increasing and continuous differentiable functions in $[0, T)$ which possess the same tail behaviors, it is also reasonable to employ the mean value theorem and impose that they coincide at time lag T , i.e.,

$$H_{\Delta}(T) = \frac{1}{\Theta} \int_0^{\Theta} H_u(T) du, \quad (52)$$

which always has a unique solution in $(0, \Theta]$. In other words, with (52) Δ can be implied from the kernel parameters κ and d and the time-to-maturity T . In particular, because the quotient $\Theta H_{\Delta} / \int_0^{\Theta} H_u du$ is bounded and converges to 1 towards infinity it is understood that a larger maturity T enhances the accuracy of (52). Although (52) can oftentimes be solved numerically with little effort, its solution is easily determined by inverting (14) and

¹⁰The reason behind choosing call options for this empirical study is that the call pricing formula (44) is more complicated than those of volatility swaps and put options (37) and (43).

we obtain the following preferable functional form,

$$\Delta = \begin{cases} (\Gamma(d)(Q - \theta e^{-\kappa\tau}) + \tau^{d-1})^{1/(d-1)} - T & \text{if } -\frac{\log(Q/\theta)}{\kappa} < \tau, \\ -\frac{\log(Q/\theta)}{\kappa} - T & \text{if } -\frac{\log(Q/\theta)}{\kappa} \geq \tau, \end{cases} \quad (53)$$

where¹¹

$$Q = \begin{cases} \frac{(T + \Theta)^d - T^d - d\tau^{d-1}\Theta}{\Gamma(d+1)\Theta} + \theta e^{-\kappa\tau} & \text{if } \tau > T + \Theta, \\ \frac{1}{\Theta} \left(\frac{d\tau^{d-1}(T - \tau) - T^d + \tau^d}{\Gamma(d+1)} + (\tau - T)\theta e^{-\kappa\tau} - \frac{\theta(e^{-\kappa\tau} - e^{-\kappa(T+\Theta)})}{\kappa} \right) & \text{if } T < \tau \leq T + \Theta, \\ \frac{\theta(e^{-\kappa T} - e^{-\kappa(T+\Theta)})}{\kappa\Theta} & \text{if } \tau \leq T. \end{cases} \quad (54)$$

Here $\theta = -((2-d)/(e\kappa))^{d-2}/(\kappa\Gamma(d-1))$ and $\tau = (2-d)/\kappa$.

Since V can only have upward jumps under (6) which already necessarily generate a strictly positive long-term mean, we will fix $\bar{V} = 0$ to lift calibration burden¹². Another benefit from this assumption is that, for the prolonged average forward volatility $I_0^2(T + \Delta)$, by referring to (22) we have a one-to-one correspondence to the observed forward variance $I_0^2(\Delta)$,

$$I_0^2(T + \Delta) = e^{-\kappa T} \left(I_0^2(\Delta) - \xi_1 \left(s \left(\frac{s^{d-1} - d\tau^{d-1}}{\Gamma(d+1)} + \theta e^{-\kappa\tau} \right) \Big|_{s=0}^{\min\{\tau, \Delta\}} + \frac{\theta e^{-\kappa s}}{\kappa} \Big|_{s=\min\{\tau, \Delta\}}^{\Delta} \right) \right. \\ \left. + \xi_1 \left(s \left(\frac{s^{d-1} - d\tau^{d-1}}{\Gamma(d+1)} + \theta e^{-\kappa\tau} \right) \Big|_{s=0}^{\min\{\tau, T+\Delta\}} - \frac{\theta e^{-\kappa s}}{\kappa} \Big|_{s=\min\{\tau, T+\Delta\}}^{T+\Delta} \right) \right), \quad (55)$$

where the equality follows directly from (64) and $\xi_1 = a\Gamma(1-c)/b^{1-c}$, and which involves no additional parameters.

We recognize the difficulty of reliably calibrating the family parameter c within the unit interval due to the variability of the hypergeometric functions near the endpoints (see Corollary 1). For this reason, we only focus on three particular values: $c = 0.3$, $c = 0.5$ (inverse Gaussian), and $c = 0.8$, and our calibration exercise will be with respect to at most four parameters: $a > 0$, $b > 0$, $\kappa > 0$ and $d \in (1/2, 1)$. More specifically, for each fixed c we minimize the mean absolute error (MAE) between the observed market prices of the call options (denoted \check{C}_0 's) and the corresponding model prices, so that the optimal parameter set is given by

$$(\hat{a}, \hat{b}, \hat{\kappa}, \hat{d}) = \underset{a>0, b>0, \kappa>0, d \in (1/2, 1)}{\operatorname{argmin}} \sum_{K, T} |\check{C}_0 - C_0^{(1,1,(a))}|,$$

where the sum acts over all available strike prices and maturities.

¹¹With $Q := \int_0^\Theta H_u(T) du / \Theta$, derivation of (54) is substantially no different from that of Corollary 1 in Section 8.3, hence omitted.

¹²As will be seen in the next section this assumption indeed does not seriously affect the calibration quality. On the other hand, without this assumption \bar{V} will show up in (55) as a parameter to be considered for calibration.

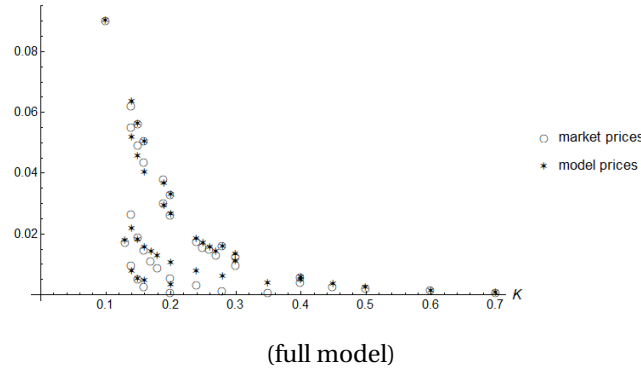
5.2 Calibration exercise

Calibration is done jointly taking into account all four different maturities for the entire data set. For contrast analysis we also consider two reduced models without mean reversion or path roughness, i.e., with $\kappa \searrow 0$ and $d \nearrow 1$, respectively. Table 1 and Table 2 below present the calibration results, where the CPU time measured in seconds¹³ are displayed as well.

Table 1: Calibration results (rounded to 6 significant figures)

c	Subgroup	\hat{a}	\hat{b}	$\hat{\kappa}$	\hat{d}	MAE	CPU time
0.3	full model	0.462174	2.21264	4.18619	0.824694	0.16747%	4770.73
	$\kappa \searrow 0$	0.161312	6.63317	-	0.72906	0.210348%	2943.19
	$d \nearrow 1$	0.471982	3.66653	4.88504	-	0.200025%	1496.14
0.5	full model★	0.16769	1.45086	2.42958	0.813053	0.162284%	6551.56
	$\kappa \searrow 0$	0.0755274	4.08084	-	0.864891	0.247694%	5338.33
	$d \nearrow 1$	0.227268	2.1441	5.45948	-	0.19279%	1234.11
0.8	full model	0.0340246	0.528195	2.78655	0.721271	0.257787%	4197.03
	$\kappa \searrow 0$	0.0114012	1.09509	-	0.532619	0.381382%	1625.84
	$d \nearrow 1$	0.0725865	9.80214	4.22903	-	0.539611%	856.578

It is seen that inclusion of mean reversion and path roughness has led to significant improvement of the model fit compared to the traditional Lévy-driven Ornstein-Uhlenbeck model with $d \nearrow 1$. If one disregards mean reversion, the model fit becomes highly labile, largely altering the calibrated fraction parameter \hat{d} , whereas the fit is still not too much worse because the selected VIX options do not have very long maturities. Also, the calibrated basic parameters \hat{a} and \hat{b} are quite different if the family parameter c has shifted, which can be easily told from the expression of the first moment ξ_1 . These results in general confirm the validity of the type-III kernel, in association with the desirable closed-form characteristic function. The model with the best fit (marked “★”) also agrees with the rapid mean-reverting nature and roughness of the volatility of S&P500 returns in reality. Under this model, the formula (53) implies $\Delta = 0.0404105$ year given the longest maturity $T = 168$ days, which is only about 15 days.



¹³The constrained optimization program is written in Mathematica® ([Wolfram Research Inc., 2015] [36]) and run on a personal laptop computer with an Intel(R) Core(TM) i5-7200 CPU @ 2.50GHz 2.71GHz.

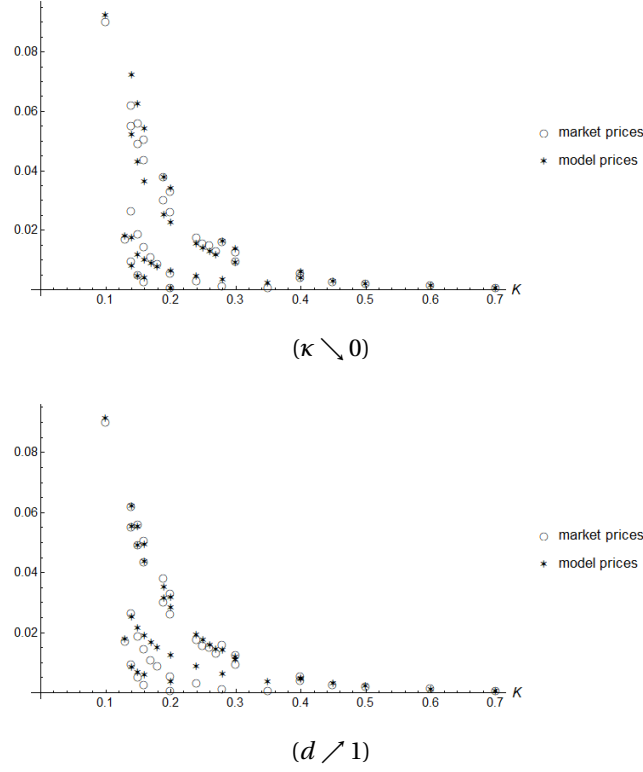


Figure 4: VIX call option prices (market vs model)

For the subgroup $c = 0.5$, the model fits are further visualized in Figure 4. Observationally, in each plot there are four strings of option prices, with an outer one having a longer time-to-maturity T . For the in-the-money options and short maturities, the two reduced models without mean reversion or roughness seem to fit quite well, as volatility jumps are already captured by X , while by incorporating mean reversion and roughness simultaneously the full model outperforms the two reduced models mainly for the deeply out-of-the-money options and long maturities. We also note the existent discrepancy between the model prices and the market prices, which we ascribe further to the presence of clustering in the instantaneous volatility process (see Section 6). We also remark that this empirical exercise only demonstrates one extremal version of the type-III kernel defined in (14), and in general one need not take θ to be the lower bound in (16) but can increment it by any arbitrary positive number, and τ takes its original form in (17) which has two distinct values. In this case, calibration will be roughly twice more computationally intense due to increased formula complexity, which in turn reflects the elegance of (18).

5.3 Power sensitivity analysis

In this section we investigate the sensitivity of the pricing and hedging of power-type volatility derivatives for the VIX index with respect to varying power coefficients, by using the general formulae proposed in Section 4. Based on the previous data set, for simplic-

ity we look at only one strike price $K = 0.2$ and suppose $T = 1$ year, after adopting the calibrated parameters under the full model with $c = 0.5$ in Table 1.

First, to ease comparison between asymmetric power and symmetric power types we assume for the power coefficients that $p_1 = p_2 = p \in [0.5, 1.5]$ and plot the price changes ($C_0^{(p,p,(a))}$, $P_0^{(p,p,(a))}$, $C_0^{(p,(s))}$ and $P_0^{(p,(s))}$) of corresponding power-type derivatives in Figure 5 and the same thing is done for the hedge changes ($\Delta(C_0^{(p,p,(a))})$, $\Delta(P_0^{(p,p,(a))})$, $\Delta(C_0^{(p,(s))})$ and $\Delta(P_0^{(p,(s))})$). For the infinite series in Proposition 6 and Corollary 4 we use the approximation $\sum_{k=0}^4$ which universally leads to a global error less than 1%. Plots for power swaps are excluded as they are already embodied in the call option pricing formulae. It is seen that, in terms of risk adjustment, the symmetric power options are able to provide much severer leverage effect for the VIX index compared to the asymmetric power options (with identical power coefficients), despite that the latter are much easier to handle in general. Also, hedges for the symmetric power options are in comparison more sensitive to changes in the power coefficient.

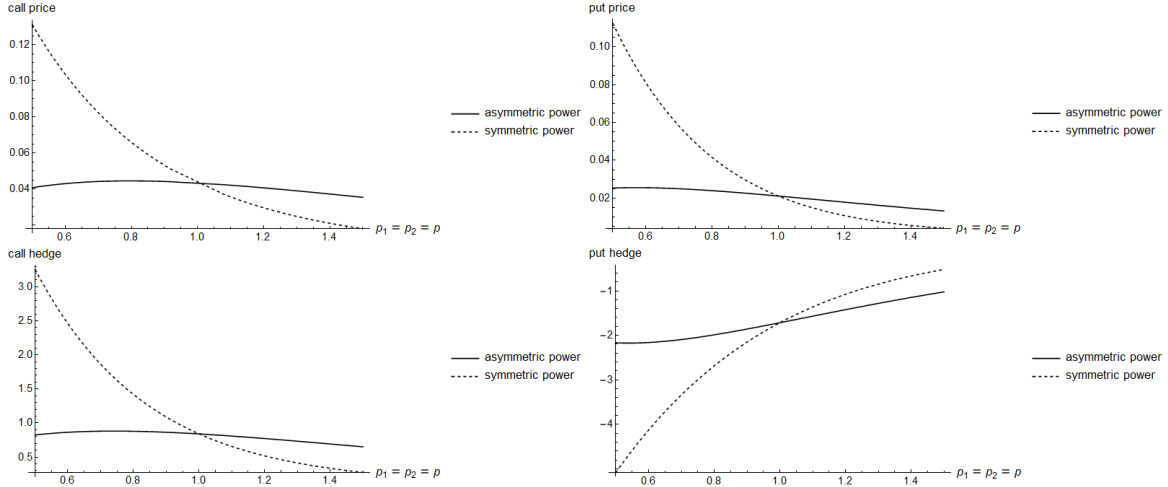


Figure 5: Power impact on VIX option prices and hedges

Of course, for an asymmetric power option, by letting the two power coefficients vary independently we can generate a power surface for its price ($C_0^{(p_1,p_2,(a))}$ and $P_0^{(p_1,p_2,(a))}$) and hedge ($\Delta(C_0^{(p_1,p_2,(a))})$ and $\Delta(P_0^{(p_1,p_2,(a))})$) which cannot be realized for symmetric power ones. For a better illustration we further restrict $p_1, p_2 \in [0.9, 1.1]$ which ensures that the powered spot VIX and strike price are not too distant from each other. Apart from showing the magnificent impact of powers on the VIX option price and hedges, these are also a reliable indicator that the general pricing-hedging formulae can be implemented fairly efficiently.

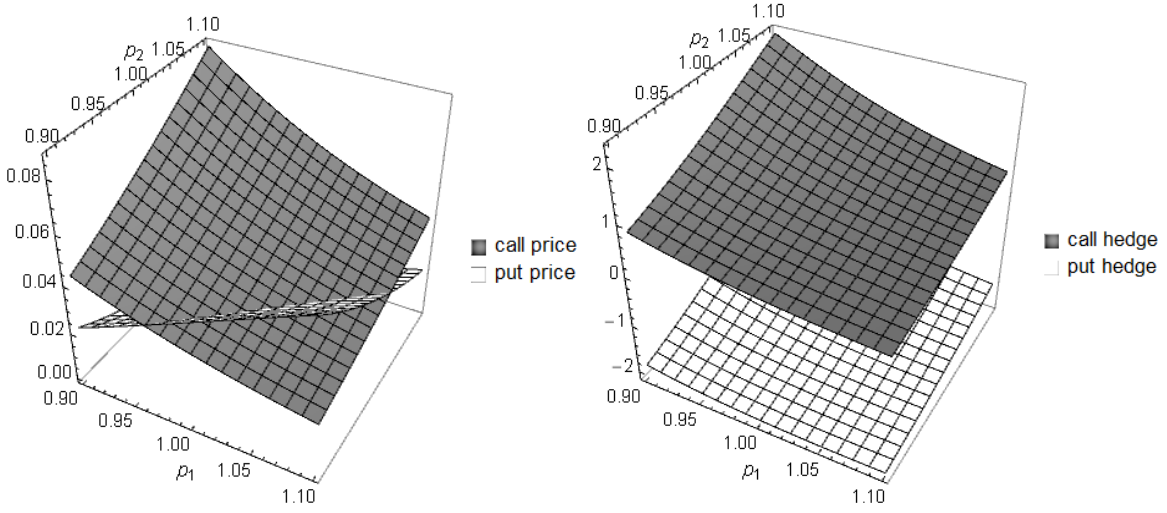


Figure 6: Asymmetric power surfaces for VIX option prices and hedges

6 Extension to rough volatility of volatility

Needless to say, the discovery of [Da Franseca & Zhang, 2019] [7] provides yet another very interesting implication, that the volatility of the average forward volatility, such as the VVIX index, also possesses rough sample paths aside from being stochastic. Although it is noticeably challenging to establish a comfortable framework coalescing both aspects of roughness, we will briefly discuss how the foregoing pricing problems may be tackled inheriting the structure of (25). For that purpose we recall the setting of Section 2.3 and define the composite process

$$\tilde{I}_t(\Delta) := I_{\mathcal{T}_t}(\Delta), \quad t \geq 0, \quad (56)$$

with

$$\mathcal{T}_t := \int_0^t Y_s^{(\eta)} ds, \quad (57)$$

where $\mathcal{T}_0 = 0$ and $Y \equiv (Y_t)$ is an \mathbb{F} -adapted square-integrable Lévy subordinator and η a kernel which respectively resemble X and h up to different parameters. The construction (56) emulates the initiative work of [Carr and Wu, 2004] [5] on stochastic time change, which has a fundamental root in the famous Dambis-Dubins-Schwartz theorem. Clearly, $Y^{(\eta)} = \int_0^\cdot \eta(\cdot, s) dY_s$ is a mean-reverting process that introduces frictions into the volatility of the average forward volatility and, if η is associated with a fraction parameter less than 1, say $d' \in (1/2, 1]$, then Proposition 1 informs us that $\sqrt{Y^{(\eta)}}$ also captures volatility-of-volatility jumps. By convention we assume independence between X and Y .

Under (56), we are able to at least write the unconditional characteristic function¹⁴ of the time-changed average forward variance in terms of nested integrals.

¹⁴Evaluating the conditional characteristic function on \mathcal{F}_{t_0} for some $t_0 \in [0, t]$ in the presence of time change can be cumbersome.

Proposition 7. Let $\phi_{Y_1}(l) := \mathbb{E}[e^{ilY_1}]$, $l \in \mathbb{R}$, denote the characteristic function of Y_1 . Then, for any $t > 0$,

$$\begin{aligned} \tilde{\phi}_t(l; \Delta) &:= \mathbb{E}[e^{il\tilde{I}_t^2(\Delta)}] \\ &= \frac{1}{\pi} \int_0^\infty \phi_{0,y}(l; \Delta) \int_0^\infty \operatorname{Re} \left[\exp \left(-i\lambda y + \int_0^t \log \phi_{Y_1} \left(\lambda \int_s^t \eta(v, s) dv \right) ds \right) \right] d\lambda dy, \quad l \in \mathbb{R}, \end{aligned} \quad (58)$$

where $\phi_{0,y}(l; \Delta)$ is as given in (26).

Note that the innermost integral in (58) can be expressed explicitly if η is any of the three types of kernels specified before, while the other three integrals remain numerical in nature. In particular, the outer two integrals are generally not interchangeable, i.e., one cannot apply the Fubini theorem and has to compute them in proper order.

Regardless, we can put (58) into the pricing formulae proposed in Section 4 to compute the prices of power volatility derivatives at time 0. However, since there are at least four numerical integrals involved, coming up with a robust calibration scheme will be an arduous task. As a means of reducing calibration burden in this connection, one should perhaps conduct characteristic function-based estimation (see [Yu, 2004] [40]) based on volatility-of-volatility index data for the parameters of Y beforehand.

7 Concluding remarks

The modeling of rough volatility is not inherently confined to Brownian sample paths and can be alternatively incorporated into a purely discontinuous Lévy process, which is also able to capture volatility jumps. Importantly, the latter approach aims to balance between the empirical findings of [Gatheral et al, 2018] [11] and [Todorov and Tauchen, 2011] [34].

The pricing-hedging framework presented in this paper is expressly tailored for volatility derivatives and built upon an Ornstein-Uhlenbeck structure with a generalized integrable kernel to establish short-term dependence. The advantage of this framework lies in the unconditional positivity of the instantaneous variance, which nullifies any consideration of the logarithm of volatility, so that integration is facilitated leading eventually to a semi-closed characteristic function for the conditional forward variance. By further inspecting the structure of this characteristic function, we discover a family of stationary kernels, classified as type-III, under which full explicitness can be achieved, and this beyond doubt lays the foundation for efficient model calibration in practice.

Since a volatility derivative is equivalent to a similar derivative written on the corresponding variance raised to the power half, it is natural to think of a wider class of power-type volatility derivatives as also a means of introducing leverage effect into the option payoffs. This is very much analogous to the original invention of power options written

Even if both η and h are exponential kernels posing no roughness, the time-changed process $\tilde{I}^2(\Delta)$ cannot be Markovian with respect to the filtration \mathbb{F} jointly generated by X and Y .

on equity prices. The general pricing-hedging formulae proposed in Section 4 should be interpreted as model-independent which require nothing more than a semi-closed model characteristic function, and will certainly work without problems for familiar models with path roughness unaccounted for. In addition, compared to the existing equity-option pricing formulae that appeared in [Bakshi and Madan, 2000] [2], these formulae are inevitably more complicated where exponential functions are mostly replaced by incomplete gamma functions. However, their applicability and efficiency remain much unaffected as demonstrated by the empirical study on VIX options.

Needless to say, by the lack of distributional stability the use of a jump model circumvents consideration of the correlation between the instantaneous volatility and the price process it is attached to. For this reason, if one's ultimate goal is to deal with traditional equity options with rough volatility, the framework established in this paper may not be a convenient one. On the other hand, if one's interests specifically start with volatility quantities, this framework then provides some new insights into how pricing and hedging may be done more efficaciously as well as, intriguingly, the potential of introducing rough volatility of volatility through a time composition process. In this connection, it is still part of our ongoing research to explore the relative importance of volatility jumps and price-volatility correlation under rough volatility models for various classes of asset prices. A future research could also be devoted to an all-around comparison of the empirical performances with the three different types of kernels, despite that their similarity has been briefly discussed in Section 2.2; of course, for the first two types model calibration will be understandably much slower because of more than one numerical integral to carry out.

8 Proofs

8.1 Proof of Proposition 1

For V defined in (6) we focus on the stochastic integral part, namely $X^{(h)}$, the rest being obviously continuous and of finite variation. Since h is continuously differentiable and $h(t+u, t) = O(e^{-\kappa u} u^{(d-1)^+}) = o(u^{d-1})$ as $u \rightarrow \infty$ for any $t \geq 0$, by the extreme value theorem there exist two positive constants $\mathfrak{b}_h \geq \mathfrak{a}_h > 0$, which depend only on the parameters of h including κ and d , such that, for any $u > 0$ and $t \in [0, T]$,

$$\mathbb{E}[(X_{t+u}^{(h)} - X_t^{(h)})^2] \in \mathbb{E}[(X_{t+u}^{(g)} - X_t^{(g)})^2] \times [\mathfrak{a}_h, \mathfrak{b}_h], \quad (59)$$

where g is the Riemann-Liouville kernel (3) with the same fraction parameter d . This relation enables us to restrict our analysis to the Riemann-Liouville fractional Lévy subordinator $X^{(g)}$ without mean reversion. The expectation on the right-hand side of (59) is then by the Lévy-Itô isometry

$$\begin{aligned} \mathcal{E}_{t,u}^{(g)} &:= \mathbb{E}[(X_{t+u}^{(g)} - X_t^{(g)})^2] \\ &= \frac{\xi_2}{\Gamma^2(d)} \left(\int_0^t ((t+u-s)^{d-1} - (t-s)^{d-1})^2 ds + \int_t^{t+u} (t+u-s)^{2(d-1)} ds \right). \end{aligned}$$

In particular, for $d > 2$ there is the fundamental Riemann-integral representation $X_t^{(g)} = \int_0^t (\int_0^s (s-v)^{d-2} / \Gamma(d-1) dX_v) ds$ due to (4) and so we only need to consider $d \leq 2$.

Suppose $d \in (1, 2]$. We observe that the obviously uniformly continuous map

$$\mathbb{R}_{++} \ni u \mapsto \frac{1}{\Gamma^2(d)} \int_0^t ((t+u-s)^{d-1} - (t-s)^{d-1})^2 ds \in \mathbb{R}_{++} \quad (60)$$

is increasing and convex for every $t > 0$, hence the only need to compare its tail behaviors against power-law tails. It is not difficult to see

$$\int_0^t ((t+u-s)^{d-1} - (t-s)^{d-1})^2 ds = O(u^{2(d-1)}) = o(u^{2d-1}), \quad \text{as } u \rightarrow \infty,$$

and

$$\int_0^t ((t+u-s)^{d-1} - (t-s)^{d-1})^2 ds = O(u^{\min\{2d-1, 2\}}), \quad \text{as } u \searrow 0,$$

which imply that

$$\int_0^t ((t+u-s)^{d-1} - (t-s)^{d-1})^2 ds \leq c_d u^{\min\{2d-1, 2\}}, \quad \forall u > 0, t \in [0, T],$$

for some constant $c_d > 0$ depending only on d . On the other hand, $\int_t^{t+u} h^2(t+u, s) ds = u^{2d-1} / ((2d-1)\Gamma(d))$. Combining things we obtain

$$\mathcal{E}_{t,u}^{(g)} \leq \frac{\xi_2}{\Gamma^2(d)} \left(c_d + \frac{1}{2d-1} \right) u^{\min\{2d-1, 2\}}. \quad (61)$$

Since the power of u in (61) strictly exceeds 1, we apply the Kolmogorov-Čentsov theorem (see, e.g., [Karatzas and Shreve, 1991, Sect. 2.2.B] [18]) [18] to conclude that $X^{(g)}$, and hence V due to (59), admits an a.s. continuous modification over \mathbb{R}_+ ; in particular, the modification is a.s. locally Hölder-continuous for every exponent in $(0, \min\{d-1, 1/2\})$.

Furthermore, using the uniform time partition \mathbf{T}_M (with $t_0 = 0$) in (32) of the interval $[0, T]$, we define the \mathbf{T}_M -quadratic variation

$$Q_M([0, T]) := \sum_{n=1}^M (X_{nT/M}^{(g)} - X_{(n-1)T/M}^{(g)})^2 \geq 0, \quad M \in \mathbb{N}_{++}, M \gg 1.$$

If $d \in (1, 2]$, by the convexity of (60) and the upper bound (61) we have

$$\begin{aligned} \mathbb{E}[Q_M([0, T])] &\leq M \mathcal{E}_{(M-1)T/M, T/M}^{(g)} \\ &\leq \frac{\xi_2}{\Gamma^2(d)} \left(c_d + \frac{1}{2d-1} \right) \left(\frac{M}{T} \right)^{\max\{2(1-d), -1\}} \rightarrow 0, \quad \text{as } M \rightarrow \infty, \end{aligned}$$

which by nonnegativity and the relation (59) implies that V has a.s. zero quadratic variation over $[0, T]$ and completes the proof of assertion (i).

Now suppose $d \in (1/2, 1]$, and then in the same vein we see that the map (60) is increasing and concave and behaves like $O(u^{2d-1})$ both as $u \rightarrow \infty$ and as $u \searrow 0$. Therefore, there exists $c_d > 0$ such that

$$\mathcal{E}_{t,u}^{(g)} \geq \frac{\xi_2}{\Gamma^2(d)} \left(c_d + \frac{1}{2d-1} \right) u^{2d-1}.$$

Note that in this case there is no way to apply the Kolmogorov-Čentsov theorem. Let X_- denote the càglàd modification of X and set

$$E := \{\omega \in \Omega : (X_t - X_{t-})(\omega) > 0, \exists t \in [0, T]\}.$$

With $\nu(\mathbb{R}_{++}) = \infty$, it is a familiar result (see again [Lyasoff, 2017, Sect. 16] [22]) that $\mathbb{P}E = 1$. Then we observe that

$$X_t^{(h)} - X_{t-}^{(h)} = \int_0^{t-} (h(t, s) - h(t-, s)) dX_s + \int_{t-}^t h(t, s) dX_s, \quad t \geq 0. \quad (62)$$

Since, for any $s \in [0, t)$, $\mathbb{R}_{++} \ni t \mapsto h(t, s) \in \mathbb{R}_+$ is a continuous map with $d \in (1/2, 1]$, by the dominated convergence theorem the first integral in (62) is naught (in the sense of L^2 -convergence) and

$$\int_{t-}^t h(t, s) dX_s = h(t, t-)(X_t - X_{t-}).$$

In consequence, there must exist some $t > 0$ such that $X_t^{(h)} - X_{t-}^{(h)} \propto h(t, t-)$. To put it another way,

$$E \subseteq \{\omega \in \Omega : (X_t^{(h)} - X_{t-}^{(h)})(\omega) \propto h(t, t-), \exists t \in [0, T]\}. \quad (63)$$

By (7) further, if $d = 1$ then h is uniformly bounded so that $h(t, t-) > 0$ for any $t > 0$, and hence (63) proves the a.s. discontinuity of the sample paths of $X^{(h)}$. In this case, since $X^{(h)}$ has no Brownian part, its quadratic variation is given by the sum of its squared jumps,

$$\sum_{t \in [0, T]} (X_t^{(h)} - X_{t-}^{(h)})^2 = \sum_{t \in [0, T]} h^2(t, t-)(X_t - X_{t-})^2 > 0, \quad \mathbb{P}\text{-a.s.},$$

where the inequality follows from the finiteness of $\sum_{t \in [0, T]} (X_t - X_{t-})^2 > 0$. On the other hand, if $d < 1$, then $h(t, t-) = \infty$ for any $t > 0$, which with (63) gives the a.s. discontinuity and unboundedness of the sample paths of $X^{(h)}$, and hence V , over $[0, T]$. An immediate implication is therefore that the sample paths of V have infinitely large squared jumps over $[0, T]$ a.s., which lead to its (a.s.) infinite quadratic variation. Therefore assertions (ii) and (iii) are proved. \square

8.2 Proof of Proposition 2

According to (22) and (25) we can write for $0 \leq t_0 < t < T$

$$I_t^2(\Delta) = V_0 e^{-\kappa(t+\Delta)} + \bar{V}(1 - e^{-\kappa(t+\Delta)}) + X_{t_0}^{(H_{t-t_0+\Delta})} + \xi_1 \int_t^{t+\Delta} H_\Delta(t, s) ds + \int_{t_0}^t H_\Delta(t, s) dX_s$$

$$= I_{t_0}^2(t - t_0 + \Delta) - \xi_1 \int_{t_0}^t H_\Delta(t, s) ds + \int_{t_0}^t H_\Delta(t, s) dX_s, \quad (64)$$

where on the right-hand side $\int_{t_0}^t H_\Delta(t, s) dX_s$ is independent from \mathcal{F}_{t_0} while the other terms are measurable with respect to \mathcal{F}_{t_0} . Therefore, by the independence lemma,

$$\mathbb{E}[e^{ilI_t^2(\Delta)} | \mathcal{F}_{t_0}] = \exp\left(il\left(I_{t_0}^2(t - t_0 + \Delta) - \xi_1 \int_{t_0}^t H_\Delta(t, s) ds\right)\right) \mathbb{E}[e^{il \int_{t_0}^t H_\Delta(t, s) dX_s}], \quad l \in \mathbb{R}.$$

For the last expectation we note that the process $\int_{t_0}^\cdot H_\Delta(\cdot, s) dX_s$ has independent increments on (t_0, T) and use the infinite divisibility of the law of X_1 to write

$$\mathbb{E}[e^{il \int_{t_0}^t H_\Delta(t, s) dX_s}] = \prod_{t_0}^t \mathbb{E}[e^{il H_\Delta(t, s) X_1}]^{ds} = \exp \int_{t_0}^t \log \mathbb{E}[e^{il H_\Delta(t, s) X_1}] ds,$$

where $\prod[\cdot]$ denotes the geometric integral operator (see, e.g., [Slavík, 2007] [31]) and which yields the desired integral representation (26). \square

8.3 Proof of Corollary 1

Proving the corollary is purely a matter of computation. If h is as in (14), then we can write

$$H_\Delta(t, s) = h(t - s + \Delta) = \begin{cases} h_-(t - s + \Delta), & \text{if } t - s + \Delta < \tau, \\ h_+(t - s + \Delta), & \text{if } t - s + \Delta \geq \tau, \end{cases} \quad (65)$$

and

$$h_-(t - s + \Delta) := \frac{(t - s + \Delta)^{d-1} - \tau^{d-1}}{\Gamma(d)} + \theta e^{-\kappa \tau} \quad \text{and} \quad h_+(t - s + \Delta) = \theta e^{-\kappa(t - s + \Delta)}.$$

Straightforward integration of (65) over the interval $[t_0, t]$ thus leads to

$$\begin{aligned} & \int_{t_0}^t H_\Delta(t - s) ds \\ &= \begin{cases} \int_{t_0}^t h_-(t - s + \Delta) ds & \text{if } \tau > t - t_0 + \Delta, \\ \int_{\min\{t + \Delta - \tau, t\}}^t h_-(t - s + \Delta) ds + \int_{t_0}^{\min\{t + \Delta - \tau, t\}} h_+(t - s + \Delta) ds & \text{if } \tau \leq t - t_0 + \Delta \end{cases} \\ &= \begin{cases} \int_{\Delta}^{t - t_0 + \Delta} h_-(s) ds & \text{if } \tau > t - t_0 + \Delta, \\ \int_{\Delta}^{\max\{\tau, \Delta\}} h_-(s) ds + \int_{\max\{\tau, \Delta\}}^{t - t_0 + \Delta} h_+(s) ds & \text{if } \tau \leq t - t_0 + \Delta \end{cases} \\ &= \begin{cases} s \left(\frac{s^{d-1} - d\tau^{d-1}}{\Gamma(d+1)} + \theta e^{-\kappa \tau} \right) \Big|_{s=\Delta}^{t - t_0 + \Delta} & \text{if } \tau > t - t_0 + \Delta, \\ s \left(\frac{s^{d-1} - d\tau^{d-1}}{\Gamma(d+1)} + \theta e^{-\kappa \tau} \right) \Big|_{s=\Delta}^{\max\{\tau, \Delta\}} - \frac{\theta e^{-\kappa s}}{\kappa} \Big|_{s=\max\{\tau, \Delta\}}^{t - t_0 + \Delta} & \text{if } \tau \leq t - t_0 + \Delta, \end{cases} \end{aligned}$$

where the second equality uses the substitution $s \mapsto t - s + \Delta$ and $\int_{\Delta}^{\max\{\tau, \Delta\}} \equiv 0$ if $\Delta \geq \tau$.

Similarly, for the second Riemann integral in (26) we have with the characteristic exponent (5) that $\xi_1 = a\Gamma(1-c)/b^{1-c}$ and that

$$\int_{t_0}^t \log \phi_{X_1}(lH_{\Delta}(t-s))ds \quad (66)$$

$$= \begin{cases} \int_{\Delta}^{t-t_0+\Delta} \log \phi_{X_1}(lh_{-}(s))ds & \text{if } \tau > t - t_0 + \Delta, \\ \int_{\Delta}^{\max\{\tau, \Delta\}} \log \phi_{X_1}(lh_{-}(s))ds + \int_{\max\{\tau, \Delta\}}^{t-t_0+\Delta} \log \phi_{X_1}(lh_{+}(s))ds & \text{if } \tau \leq t - t_0 + \Delta. \end{cases} \quad (67)$$

Since the integrands in (66) are obviously integrable over the designated domains, it only suffices to consider the indefinite integrals, $\mathcal{J}_{+}(s) := \int (b - ile^{-\kappa s})^c ds$ and $\mathcal{J}_{-}(s) := \int (b - ils^{d-1})^c ds$. Note that $a\Gamma(-c)$ is just a scaling factor while the integration of b^c is immediate. For \mathcal{J}_{+} , we observe by using binomial expansion that

$$\begin{aligned} \mathcal{J}_{+}(s) &= (-1)^{c+1} (il)^c \sum_{k=0}^{\infty} \binom{c}{k} \left(-\frac{b}{il}\right)^k \frac{e^{-\kappa(c-k)s}}{\kappa(c-k)} \\ &= \frac{(-1)^{c+1} (il)^c e^{-\kappa cs}}{c\kappa} \sum_{k=0}^{\infty} \frac{(-c)_k^2}{(1-c)_k} \left(\frac{be^{\kappa ks}}{il}\right)^k \\ &= \frac{(-1)^{c+1} (il)^c e^{-\kappa cs}}{c\kappa} {}_1F_2\left(-c, -c; 1-c; \frac{be^{\kappa ks}}{il}\right), \end{aligned}$$

where $(\cdot)_\cdot$ denotes the Pochhammer symbol, a.k.a. the rising factorial, and which after simplification leads to (30). The case of \mathcal{J}_2 is slightly more involved but can be proved in a similar fashion, and we obtain

$$\mathcal{J}_{-}(s) := s \left(\left(b - ile^{-\kappa \tau} + \frac{il\tau^{d-1}}{\Gamma(d)} \right)^c {}_2F_1\left(-c, \frac{1}{d-1}, \frac{d}{d-1}; \frac{ils^{d-1}}{il\tau^{d-1} + (b - ile^{-\kappa \tau})\Gamma(d)}\right) \right),$$

thus yielding (31). Putting these together we arrive at (29). \square

8.4 Proof of Proposition 3

First notice that

$$\mathbb{E}[\check{V}_{nT/M}] = V_0 e^{-\kappa nT/M} + \bar{V}(1 - e^{-\kappa nT/M}) + \xi_1 \sum_{k=0}^{n-1} h\left(\frac{nT}{M}, \frac{kT}{M}\right) \frac{T}{M}.$$

For a given $t \in (0, T]$, we choose $n \equiv n(t, M) = \lfloor Mt/T \rfloor$, so that $\lim_{M \rightarrow \infty} (n(t, M)T/M) = t$. Since the Riemann integral $\int_0^t h(t, s)ds$ is well-defined for $t \in [0, T]$, (33) constitutes a conventional rectangular Riemann-sum approximation and it is familiar that

$$\mathbb{E}[\check{V}_{n(t, M)T/M} - V_t] = O(M^{-1}), \quad \text{as } M \rightarrow \infty. \quad (68)$$

This shows asymptotic unbiasedness. In addition to (68), using the relation

$$\mathbb{E}[(\check{V}_{n(t,M)T/M} - V_t)^2] = \mathbb{E}[\check{V}_{n(t,M)T/M} - V_t]^2 + \text{Var}[\check{V}_{n(t,M)T/M}],$$

for proving the L^2 -convergence rate it is sufficient to note that, in the same vein,

$$\begin{aligned} M\text{Var}[\check{V}_{n(t,M)T/M}] &= T(\xi_2 - \xi_1^2) \sum_{k=0}^{n(t,M)-1} h^2\left(\frac{n(t,M)T}{M}, \frac{kT}{M}\right) \frac{T}{M} \\ &\rightarrow T(\xi_2 - \xi_1^2) \int_0^t h^2(t, s) ds, \quad \text{as } M \rightarrow \infty. \end{aligned}$$

□

8.5 Proof of Proposition 4

The relationship between fractional moments and the characteristic function of a real-valued random variable has been well established. In particular, knowing that $I_T(\Delta)$ is strictly positive with $\mathbb{E}[I_T^p(\Delta)] < \infty$ for every $p > 0$, we have ([Pilenis, 2016, Equation (2.19)] [27])

$$S_{t_0}^{(p)} = \mathbb{E}[(I_T^2(\Delta))^{p/2} | \mathcal{F}_{t_0}] = (-i)^{p/2} \phi_{t_0, T}^{(p/2)}(0; \Delta). \quad (69)$$

If p is even, then (69) is understood as a conventional derivative corresponding to the first equation in (36). Otherwise, it represents a fractional derivative and can be written ([Laue, 1980, Theorem 2.1] [20])

$$\begin{aligned} S_{t_0}^{(p)} &= \sec \frac{\pi(p/2 - \lfloor p/2 \rfloor)}{2} \frac{p/2 - \lfloor p/2 \rfloor}{\Gamma(1 - p/2 + \lfloor p/2 \rfloor)} \\ &\quad \times \text{Re} \left[(-i)^{\lfloor p/2 \rfloor} \int_{-\infty}^{\lambda} \frac{\phi_{t_0, T}^{(\lfloor p/2 \rfloor)}(\lambda; \Delta) - \phi_{t_0, T}^{(\lfloor p/2 \rfloor)}(l; \Delta)}{(\lambda - l)^{p/2 - \lfloor p/2 \rfloor + 1}} dl \Big|_{\lambda=0} \right]. \end{aligned} \quad (70)$$

Since $\phi_{t_0, T}(\cdot; \Delta) \in \mathcal{C}^{\lfloor p/2 \rfloor}(\mathbb{R})$, we can apply the dominated convergence theorem together with the substitution $l \mapsto -l$ to recast (70) as

$$\begin{aligned} S_{t_0}^{(p)} &= \sec \frac{\pi(p/2 - \lfloor p/2 \rfloor)}{2} \frac{p/2 - \lfloor p/2 \rfloor}{\Gamma(1 - p/2 + \lfloor p/2 \rfloor)} \\ &\quad \times \text{Re} \left[(-i)^{\lfloor p/2 \rfloor} \int_0^{\infty} \frac{\phi_{t_0, T}^{(\lfloor p/2 \rfloor)}(0; \Delta) - \phi_{t_0, T}^{(\lfloor p/2 \rfloor)}(-l; \Delta)}{l^{p/2 - \lfloor p/2 \rfloor + 1}} dl \right]. \end{aligned}$$

Using that $(-i)^{\lfloor p/2 \rfloor} \phi_{t_0, T}^{(\lfloor p/2 \rfloor)}(0; \Delta) = S_{t_0}^{(2\lfloor p/2 \rfloor)}$ and the Hermitian property of the characteristic function we arrive at the second equation in (36). □

8.6 Proof of Corollary 2

Based on (26), we have for $p/2 \in \mathbb{N}$ that

$$\Delta_T(\phi_{t_0, T}(l; \Delta)) = il\phi_{t_0, T}(l; \Delta),$$

so that

$$(\Delta_T(\phi_{t_0,T}(l;\Delta)))^{(p/2)} = i \left(l \phi_{t_0,T}^{(p/2)}(l;\Delta) + \frac{p \phi_{t_0,T}^{(p/2-1)}(l;\Delta)}{2} \right).$$

Sending $l \rightarrow 0$ gives the first equation in (38).

For the second equation in (38) we must justify that differentiation under Δ_T can be done inside the integral. Interchange with the real part is then simply allowed thanks to the Hermitian property. Since $\phi_{t_0,T}(\cdot;\Delta) \in \mathcal{C}^{\lfloor p/2 \rfloor}(\mathbb{R})$ and $\phi_{t_0,T}^{(\lfloor p/2 \rfloor)}(l;\Delta) = O(\phi_{t_0,T}(l;\Delta))$ as $l \rightarrow \infty$, we only need to check integrability of the tails of $\text{Re}[\phi_{t_0,T}(l;\Delta)]/l^{p/2-\lfloor p/2 \rfloor}$ for $l \geq 0$. From (64) we know that

$$\mathfrak{A} := I_{t_0}^2(T - t_0 + \Delta) - \xi_1 \int_{t_0}^T H_\Delta(t, s) ds > 0,$$

which is a known value given \mathcal{F}_{t_0} and allows us to rewrite

$$\phi_{t_0,T}(l;\Delta) = e^{il\mathfrak{A}} \varphi_{t_0,T}(l;\Delta), \quad l \in \mathbb{R},$$

where $\varphi_{t_0,T}(l;\Delta)$ is the characteristic function of the random variable $\int_{t_0}^T H_\Delta(T, s) dX_s > 0$, whose law admits a well-defined density (recall that H_Δ is continuous and v is non-atomic). Hence, we have

$$\int_0^\infty \text{Re}[e^{il\mathfrak{A}} \varphi_{t_0,T}(l;\Delta)] dl = 0,$$

which with $p/2 - \lfloor p/2 \rfloor \in (0, 1)$ for any $p \notin 2\mathbb{N}$ implies the desired tail integrability. \square

8.7 Proof of Proposition 5

Let $f_{t_0,T}(x;\Delta)$ and $F_{t_0,T}(x;\Delta)$, for $x > 0$, respectively denote the density function and the distribution function of $I_T^2(\Delta)|_{\mathcal{F}_{t_0}}$, which exist because the law of X_1 is absolutely continuous. For the price of the asymmetric power put option on $I_T(\Delta)$ at $t_0 \in [0, T)$, we adopt $\tilde{p} = p_1/2$ to rewrite its terminal payoff so that

$$\begin{aligned} P_{t_0}^{(p_1, p_2, (a))} &= \mathbb{E}[(K^{p_2} - I_T^{2\tilde{p}}(\Delta))^+ | \mathcal{F}_{t_0}] \\ &= \int_0^{K^{p_2/\tilde{p}}} (K^{p_2} - x^{\tilde{p}}) f_{t_0,T}(x) dx \\ &= K^{p_2} F_{t_0,T}(K^{p_2/\tilde{p}}; \Delta) - \int_0^{K^{p_2/\tilde{p}}} x^{\tilde{p}} f_{t_0,T}(x; \Delta) dx \\ &:= \mathfrak{E}_2 - \mathfrak{E}_1. \end{aligned}$$

Further denote $\tilde{K} = K^{p_2/\tilde{p}}$. Using the Fourier inversion formula we have

$$\mathfrak{E}_2 = K^{p_2} \left(\frac{1}{2} - \frac{1}{\pi} \int_0^\infty \text{Re} \left[\frac{e^{-i\tilde{K}l} \phi_{t_0,T}(l;\Delta)}{il} \right] dl \right)$$

and

$$\mathfrak{E}_1 = \frac{1}{\pi} \int_0^{\tilde{K}} x^{\tilde{p}} \int_0^\infty \operatorname{Re}[e^{-ilx} \phi_{t_0, T}(l; \Delta)] dl dx = \frac{1}{\pi} \int_0^\infty \operatorname{Re}\left[\phi_{t_0, T}(l; \Delta) \int_0^{\tilde{K}} e^{-ilx} x^{\tilde{p}} dx\right] dl, \quad (71)$$

where the second equality uses the Fubini theorem since the integral in x is taken over a finite interval. To evaluate the inner integral in (71), we apply the substitution $x \mapsto ilx$ and observe that

$$\begin{aligned} \int_0^{\tilde{K}} e^{-ilx} x^{\tilde{p}} dx &= (il)^{-\tilde{p}-1} \int_0^{i\tilde{K}l} e^{-x} x^{\tilde{p}} dx \\ &= (il)^{-\tilde{p}-1} \left(\int_0^\infty - \int_{i\tilde{K}l}^\infty \right) e^{-x} x^{\tilde{p}} dx \\ &= (il)^{-\tilde{p}-1} (\Gamma(\tilde{p}+1) - \Gamma(\tilde{p}+1, i\tilde{K}l)), \end{aligned}$$

where the second equality follows because the integrand is analytic over the horizontal half-strip $\{x : \operatorname{Re} x > 0, \operatorname{Im} x \in (0, \tilde{K}l)\}$ with $l > 0$. This establishes (41) after rearrangement.

The pricing formula for the similar asymmetric call option results from a standard parity argument that

$$(I_T^{p_1}(\Delta) - K^{p_2})^+ - (K^{p_2} - I_T^{p_1}(\Delta))^+ = I_T^{p_1}(\Delta) - K^{p_2},$$

together with Proposition 4. It is important to note that a single integral representation for the call price is inaccessible due to inapplicability of the Fubini theorem when integration acts over $[\tilde{K}, \infty) \ni x$. \square

8.8 Proof of Corollary 3

We simply use the bounded-ness and Hermitian property of $\phi_{t_0, T}(\cdot; \Delta)$ in order to apply Δ_T to (41) inside the real part of the integral. For the call option we use the parity relation (42). \square

8.9 Proof of Proposition 6

First consider the symmetric power put option with the payoff decomposition (48), so that we may write

$$P_{t_0}^{(p, (s))} = K^p F_{t_0, T}(K^2; \Delta) + \sum_{k=1}^{\infty} \binom{p}{k} (-1)^k K^{p-k} \tilde{\mathfrak{E}}_k$$

and for every $k \in \mathbb{N}_{++}$ using the argument in Section 8.7 we have

$$\begin{aligned} \tilde{\mathfrak{E}}_k &= \frac{1}{\pi} \int_0^\infty \operatorname{Re}\left[\phi_{t_0, T}(l; \Delta) \int_0^{K^2} e^{-ilx} x^{k/2} dx\right] dl \\ &= \frac{1}{\pi} \int_0^\infty \operatorname{Re}\left[\phi_{t_0, T}(l; \Delta) \frac{\Gamma(k/2+1) - \Gamma(k/2+1, iK^2 l)}{(il)^{k/2+1}}\right] dl. \end{aligned}$$

which obviously allows the series to be augmented to $k = 0$ and completes the proof of (50) after simplification.

For the similar symmetric call option price, we rely on the decomposition (49) to write

$$C_{t_0}^{(p,(s))} = \sum_{k=0}^{\lfloor p \rfloor} \binom{p}{k} (-K)^k \check{\mathfrak{C}}_{p-k} + \Sigma_{t_0}^{(p)},$$

where all the summands with index $k > p$ in conditional expectation are put into $\Sigma_{t_0}^{(p)}$. For every $0 \leq k < p$ note that

$$\check{\mathfrak{C}}_{p-k} = S_{t_0}^{(p-k)} - \int_0^{K^2} x^{(p-k)/2} f_{t_0,T}(x; \Delta)(x) dx,$$

so that a parity argument can be employed where the integral on the left-hand side is evaluated in the same vein as in (71). If $p \in \mathbb{N}$ then $\Sigma_{t_0}^{(p)}$ is clearly naught. On the other hand, if $p \notin \mathbb{N}$, then we write

$$\Sigma_{t_0}^{(p)} = \sum_{k=\lfloor p \rfloor + 1}^{\infty} \binom{p}{k} (-K)^k \check{\mathfrak{C}}_k,$$

where

$$\check{\mathfrak{C}}_k = \int_{K^2}^{\infty} x^{(p-k)/2} f_{t_0,T}(x; \Delta) dx = \frac{1}{\pi} \int_0^{\infty} \operatorname{Re} \left[\phi_{t_0,T}(l; \Delta) \int_{K^2}^{\infty} e^{-ilx} x^{-(k-p)/2} dx \right] dl.$$

Here the Fubini theorem applies because $k - p > 0$. At this point it suffices to observe that

$$\int_{K^2}^{\infty} e^{-ilx} x^{-(k-p)/2} dx = \frac{\Gamma(1 - (k-p)/2, iK^2 l)}{(il)^{1-(k-p)/2}},$$

which is well-defined as $p - k$ cannot be an even number. \square

8.10 Proof of Corollary 4

The proof is similar to that of Corollary 3, except that Δ_T acts on (50) and (51) termwise, where the interchange of integration and differentiation is permitted for the same reason as in Section 8.8. \square

8.11 Proof of Proposition 7

By mimicking the steps in Section 8.2, it can be deduced from (57) that the characteristic function of \mathcal{T}_t for a fixed $t > 0$ is given by

$$\phi_{\mathcal{T}_t}(l) := \mathbb{E}[e^{il\mathcal{T}_t}] = \exp \int_0^t \log \phi_{Y_1} \left(l \int_s^t \eta(v, s) dv \right) ds, \quad l \in \mathbb{R}.$$

By assumption the process Y has its own filtration $\{\sigma((Y_s)_{s \in [0, t]})\}_{t \geq 0}$ independent from that of X . Therefore, via subsequent conditioning we have¹⁵

$$\tilde{\phi}_{0,t}(l; \Delta) := \mathbb{E}[e^{iul_t^2(\Delta)}] = \mathbb{E}[\mathbb{E}[e^{iul_{\mathcal{T}_t}^2(\Delta)} | \sigma((Y_s)_{s \in [0, t]})]] = \mathbb{E}[\phi_{0, \mathcal{T}_t}(l; \Delta)]. \quad (72)$$

Since the law of the time change is absolutely continuous, (72) can be written using inverse Fourier transform as

$$\tilde{\phi}_t(l; \Delta) = \frac{1}{\pi} \int_0^\infty \phi_{0,s}(l; \Delta) \int_0^\infty \operatorname{Re}[e^{-i\lambda s} \phi_{\mathcal{T}_t}(\lambda)] d\lambda ds,$$

and this is exactly the same as (58). \square

References

- [1] Abramowitz, M. & Stegun, I.A. (1972). *Handbook of Mathematical Functions with Formulas, Graphs, and Mathematical Tables*, 10th Ed. U.S. National Bureau of Standards, Washington, D.C.
- [2] Bakshi, G. & Madan, D.B. (2000). Spanning and derivative-security valuation. *Journal of Financial Economics*, **55**: 205–238.
- [3] Bayer, C., Friz, P., & Gatheral, J. (2016). Pricing under rough volatility. *Quantitative Finance*, **16**: 887–904.
- [4] Blenman, L.P. & Clark, S.P. (2005). Power exchange options. *Finance Research Letters*, **2**: 97–106.
- [5] Carr, P. & Wu, L. (2004). Time-changed Lévy processes and option pricing. *Journal of Financial Economics*, **71**: 113–141.
- [6] Corless, R.M., Gonnet, G.H., Hare, D.E.G., Jeffrey, D.J., & Knuth, D.E. (1996). On the Lambert W function. *Advances in Computational Mathematics*, **5**: 329–359.
- [7] Da Fonseca, J. & Zhang, W. (2019). Volatility of volatility is (also) rough. *Journal of Futures Markets*, **39**: 600–611.
- [8] El Euch, O. & Rosenbaum, M. (2018). Perfect hedging in rough Heston models. *Annals of Applied Probability*, **28**: 3813–3856.
- [9] El Euch, O. & Rosenbaum, M. (2019). The characteristic function of rough Heston models. *Mathematical Finance*, **29**: 3–38.
- [10] Garnier, J. & Sølner, K. (2018). Option pricing under fast-varying and rough stochastic volatility. *Annals of Finance*, **14**: 489–516.
- [11] Gatheral, J., Jaisson, T., & Rosenbaum, M. (2018). Volatility is rough. *Quantitative Finance*, **18**: 933–949.
- [12] Gatheral, J. & Keller-Ressel, M. (2019). Affine forward variance models. *Finance and Stochastics*, **23**: 501–533.
- [13] Golub, G.H. & Welsch, J.H. (1969). Calculation of Gauss quadrature rules. *Mathematics of Computation*, **23**: 221–230.
- [14] Horvath, B., Jacquier, A., & Tankov, P. (2020). Volatility options in rough volatility models. *SIAM Journal on Financial Mathematics*, **11**: 437–469.
- [15] Jaber, E.A., Larsson, M., & Pulido, S. (2019). Affine Volterra processes. *Annals of Applied Probability*, **29**: 3155–3200.

¹⁵To compute (72) one can also simulate $Y^{(\eta)}$, using what has been discussed in Section 3.

-
- [16] Jacquier, A., Martini, C., & Muguruza, A. (2018). On VIX futures in the rough Bergomi model. *Quantitative Finance*, **18**: 45–61.
 - [17] Jost, C. (2006). Transformation formulas for fractional Brownian motion. *Stochastic Processes and their Applications*, **116**: 1341–1357.
 - [18] Karatzas, I. & Shreve, S.E. (1991). *Brownian Motion and Stochastic Calculus*, 2nd Ed. Springer-Verlag, New York.
 - [19] Küchler U. & Tappe, S. (2013). Tempered stable distributions and processes. *Stochastic Processes and their Applications*, **123**(12): 4256–4293.
 - [20] Laue, G. (1980). Remarks on the relation between fractional moments and fractional derivatives of characteristic functions. *Journal of Applied Probability*, **17**: 456–466.
 - [21] Livieri, G., Mauti, S., Pallavicini, A., & Rosenbaum, M. (2018). Rough volatility: Evidence from option prices. *IISE Transactions*, **50**: 767–776.
 - [22] Lyasoff, A. (2017). *Stochastic Methods in Asset Pricing*, MIT Press, Cambridge.
 - [23] Mandelbrot, B.B. & van Ness, J.W. (1968). Fractional Brownian motions, fractional noises and applications. *SIAM Review*, **10**: 422–437.
 - [24] Marquardt, T. (2006). Fractional Lévy processes with an application to long memory moving average processes. *Bernoulli*, **12**: 1099–1126.
 - [25] Matsui, M. & Pawlas, Z. (2016). Fractional absolute moments of heavy tailed distributions. *Brazilian Journal of Probability and Statistics*, **30**: 272–298.
 - [26] Molchan, G. & Golosov, J. (1969). Gaussian stationary processes with asymptotic power spectrum. *Soviet Mathematics Doklady*, **10**: 134–137.
 - [27] Pilenis, I. (2018). Positive-part moments via characteristic functions, and more general expressions. *Journal of Theoretical Probability*, **31**: 527–555.
 - [28] Raible, S. (2000). *Lévy Processes in Finance: Theory, Numerics, and Empirical Facts*. Dissertation zur Erlangung des Doktorgrades der Mathematischen Fakultät der Albert-Ludwigs-Universität Freiburg i. Br. 169 pages.
 - [29] Ronsiński, J. (2007). Tempering stable processes. *Stochastic Processes and their Applications*, **117**: 677–707.
 - [30] Schoutens, W. (2003). *Lévy Processes in Finance: Pricing Financial Derivatives*. John Wiley & Sons Ltd, The Atrium, Southern Gate, Chichester.
 - [31] Slavík, A. (2007). *Product Integration, its History and Applications*. Nečas Center for Mathematical Modeling & History of Mathematics, Prague.
 - [32] Takaishi, T. (2020). Rough volatility of Bitcoin. *Finance Research Letters*, **32**: 101379.
 - [33] Tikanmäki, H. & Mishura, Y. (2011). Fractional Lévy processes as a result of compact interval integral transformation. *Stochastic Analysis and Applications*, **29**: 1081–1101.
 - [34] Todorov, V. & Tauchen, G. (2011). Volatility jumps. *Journal of Business and Economic Statistics*, **29**: 356–371.
 - [35] Wang, X. (2016). Pricing power exchange options with correlated jump risk. *Finance Research Letters*, **19**: 90–97.
 - [36] Wolfram Research, Inc. (2015). *Mathematica*, Version 10.3. Champaign IL.
 - [37] Wolpert, R.L. & Taqqu, M.S. (2004). Fractional Ornstein-Uhlenbeck Lévy processes and the Telecom process: Upstairs and downstairs. *Signal Processing*, **85**: 1523–1545.
 - [38] Xia, W. (2017). Pricing exotic power options with a Brownian-time-changed variance gamma process. *Communications in Mathematical Finance*, **6**: 21–60.

- [39] Xia, W. (2019). A stochastic-volatility model for pricing power variants of exchange options. *Journal of Derivatives*, **26**: 113–127.
- [40] Yu, J. (2004). Empirical characteristic function estimation and its applications. *Econometric Reviews*, **23**: 93–123.